

UNCLASSIFIED

AD NUMBER
AD476767
NEW LIMITATION CHANGE
TO Approved for public release, distribution unlimited
FROM Distribution authorized to U.S. Gov't. agencies and their contractors; Administrative/Operational Use; Nov 1965. Other requests shall be referred to Air Force Flight Dynamics Lab., Structures Div. [FDT], Wright-Patterson AFB, OH 45433.
AUTHORITY
AFFDL ltr dtd 25 Oct 1972

THIS PAGE IS UNCLASSIFIED

AFFDL-TR-65-162

476262

STRUCTURAL TEMPERATURES AT SUPERSONIC FLIGHT FROM B-58A AND F-105D AIRCRAFT

E. DURKEE

TECHNICAL REPORT No. AFFDL-TR-65-162

NOVEMBER 1965

This document is subject to special export controls and each transmittal to foreign nationals may be made only with prior approval of the Structures Division (FDT), Air Force Flight Dynamics Laboratory, Wright-Patterson AFB, Ohio.

**AIR FORCE FLIGHT DYNAMICS LABORATORY
RESEARCH AND TECHNOLOGY DIVISION
AIR FORCE SYSTEMS COMMAND
WRIGHT-PATTERSON AIR FORCE BASE, OHIO**

NOTICES

When Government drawings, specifications, or other data are used for any purpose other than in connection with a definitely related Government procurement operation, the United States Government thereby incurs no responsibility nor any obligation whatsoever; and the fact that the Government may have formulated, furnished, or in any way supplied the said drawings, specifications, or other data, is not to be regarded by implication or otherwise as in any manner licensing the holder or any other person or corporation, or conveying any rights or permission to manufacture, use, or sell any patented invention that may in any way be related thereto.

Copies of this report should not be returned to the Research and Technology Division unless return is required by security considerations, contractual obligations, or notice on a specific document.

STRUCTURAL TEMPERATURES AT SUPERSONIC FLIGHT FROM B-58A AND F-105D AIRCRAFT

E. DURKEE

This document is subject to special export controls and each transmittal to foreign nationals may be made only with prior approval of the Structures Division (FDT), Air Force Flight Dynamics Laboratory, Wright-Patterson AFB, Ohio.

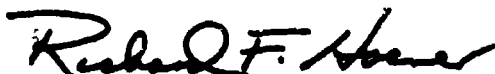
FOREWORD

This report was prepared in the Theoretical Mechanics Branch, Structures Division, Air Force Flight Dynamics Laboratory, Research and Technology Division, Wright-Patterson Air Force Base, Ohio. The graphic segments of this report were prepared by the University of Dayton Research Institute, Dayton, Ohio, under Air Force Contract Number AF33(616)-6719, Research and Development Project 1367, "Structural Design Criteria," Task 136717, "Empirical Loads Interpretation and Analysis." This project and task are part of the Air Force Systems Command's Applied Research Program 750A, "Mechanics of Flight."

The flight data used in this report were extracted from reports and data sheets which were prepared by Republic Aviation Corporation and the Convair Division of General Dynamics Corporation.

Manuscript released by the author, August 1965, for publication as a FDL Technical Report.

This technical report has been reviewed and is approved.


RICHARD F. HÖRNER
Acting Chief
Structures Division

ABSTRACT

This report presents supersonic flight data from an instrumented B-58A and F-105D aircraft. These data comprise supersonic Mach number, altitude and recorded and predicted temperatures at various wing and fuselage stations. Data presentation is in the form of curves, plots and tables with pertinent descriptive information. These findings are presented herein to provide a basis for extending the state-of-the-art in structural design criteria for current and future flight vehicles.

TABLE OF CONTENTS

<u>Section</u>		<u>Page</u>
I	Introduction	1
II	Discussion	3
2.1	Purpose	3
2.2	Weapon Systems	3
2.2.1	B-58A Aircraft Information	3
2.2.2	F-105D Aircraft Information	6
2.3	Instrumentation	8
2.3.1	B-58A Aircraft Instrumentation	8
2.3.2	F-105D Aircraft Instrumentation	10
2.4	Description of Tests	11
2.4.1	B-58A Airplane Tests	11
2.4.2	F-105D Airplane Tests	13
2.5	Discussion of Data	14
2.5.1	B-58A Airplane Test Data	14
2.5.2	F-105D Airplane Test Data	21
III	Conclusions	29
	References	31
	Appendixes	32
	Appendix I - Flight Profiles	33
	Appendix II - B-58A Aircraft Temperature Prediction Procedure	53
	Appendix III - Heat Balance Equations, F-105B	55

LIST OF FIGURES

<u>Figure</u>		<u>Page</u>
1	B-58A Aircraft with Thermocouple Locations	5
2	F-105D Aircraft	7
3	Flight Nr. 37 Profile, B-58A	34
4	Wing Station 198 Upper Surface Outer Skin Temperature, Flight 37, B-58A	35
5	Wing Station 198 Lower Surface Outer Skin Temperature, Flight 37, B-58A	36
6	Wing Stations 509 and 530 Lower Surface Outer Skin Temperature, Flight 37, B-58A	37
7	Wing Station 200 Leading Edge Temperature Flight 37, B-58A	38
8	Fuselage Stations 340 and 385 Skin Temperature, Flight 37, B-58A	39
9	Flight Nr. 48 Profile, B-58A	40
10	Wing Station 198 Upper Surface Outer Skin Temperature, Flight 48, B-58A	41
11	Wing Station 198 Lower Surface Outer Skin Temperature, Flight 48, B-58A	42
12	Wing Station 509 Upper Surface Outer Skin Temperature, Flight 48, B-58A	43
13	Wing Stations 509 and 530 Lower Surface Outer Skin Temperature, Flight 48, B-58A	44
14	Elevon Inner Flange Lower Surface Temperature, Wing Stations 545 and 575, Flight 48, B-58A	45
15	Fuselage Station 340 Skin Temperature, Flight 48, B-58A	46
16	Mach Number Temperature Profile, Fuselage Station 340, Flight 37, B-58A	47

Figure**Page**

17	Mach Number Temperature Profile, Wing Station 200, Flight 37, B-58A	48
18	Temperature Time Profile, Wing and Nose Boom, Flight 21F-4, F-105D	49
19	Temperature Mach Number Profile, Wing and Nose Boom, Flight 21F-4, F-105D	50
20	Temperature Time Profile, Wing and Nose Boom, Flight 21F-5, F-105D	51
21	Temperature Mach Number Profile, Wing and Nose Boom, Flight 21F-5, F-105D	52
A-1	Fuel Cell Floor Fuselage Station 553-581	61

LIST OF TABLES

<u>Table</u>		<u>Page</u>
1	Design Weights and Load Factors, B-58A	6
2	Design Weights and Load Factors, F-105D	8
3	Temperature Measurement Schedule, B-58A	10
4	Test Conditions, B-58A	11
5	Test Conditions, F-105D	13
6	Predicted and Measured Nacelle Former Temperatures, B-58A	21
7	Flight Test Temperature Data, F-105D	24
8	Free Stream Total Temperatures, Flight 21F-4, F-105D	26
9	Free Stream Total Temperatures, Flight 21F-5, F-105D	27

LIST OF SYMBOLS

M	Mach number
r	Temperature recovery factor
T_{to}	Stagnation temperature
T_{aw}	Adiabatic wall temperature
T_o	Free stream temperature
T	Temperature in degrees Fahrenheit
γ	Ratio of the specific heats of air

SECTION I

INTRODUCTION

The progressively increasing flight speeds of consecutive generations USAF military aircraft result in correspondingly increasing temperatures on the aircraft surface and subsequently on the interior structure. This heating of the airframe during high speed flight through the atmosphere is termed aerodynamic heating. Aerodynamic heating poses serious problems to the structural designer of supersonic and hypersonic flight vehicles, since, high temperatures in the airframe adversely affect the response of the structure to static and dynamic loads. Consequently, standard methods of stress analysis, design procedures and practices, materials selection, etc. must be modified to include thermal effects. Therefore, it is relevant to investigate procedures for predicting airframe temperatures and actual recorded airframe temperatures obtained during high speed flight.

It is the purpose of this report to present, primarily, temperature data from high speed flights of the B-58A and F-105D aircraft and as available compare these data with predicted values. This presentation of actual and predicted data is intended to verify current temperature prediction techniques,

or as required, be useful for modifying or developing new prediction techniques. In addition, the tabulation of recorded temperature data at specific Mach numbers is expected to enhance the development of structural design criteria for current and future flight vehicles.

These two diverse types of aircraft (B-58A and F-105D) are included within the scope of this report because of near identical Mach number and altitude ranges and that actual flight temperature data were available from each aircraft. The B-58A aircraft was designed and fabricated by the Convair Division of General Dynamics Corporation, Fort Worth, Texas. The F-105D aircraft was designed and fabricated by the Republic Aviation Corporation, Farmingdale, New York. Additional airplane descriptive information is contained in Section 2.2 "Weapon Systems" of this report.

SECTION II

DISCUSSION

2.1 Purpose

The B-58A and F-105D aircraft temperature loads surveys were conducted to measure structural temperatures during steady-state and transient maneuvers for comparison with predicted and design temperatures and for investigation of any unknown critical temperature that might be incurred during critical design flight conditions.

2.2 Weapon Systems

2.2.1 B-58A Aircraft Information

B-58A airplane number 4, USAF S/N 55-663, was employed to conduct a structural temperature survey. This test aircraft was structurally similar to production aircraft except, as modified to allow for test instrumentation or non-availability of standard parts at the time of fabrication. The airplane was equipped with an interim fuel system and J79-1 engines in lieu of the non-available J79-5 engines. Major structural deviations included: modified wing leading edge removable panels, single sheet construction fin leading edge and dorsal fairing, single sheet construction nacelle strut leading edge, open construction nacelle panels and modified inboard nacelle pylon plate. These structural deviations and the incomplete

flight loads survey made it mandatory to restrict the limit load factor to 80 percent of design for this test aircraft.

The B-58A aircraft, illustrated in Figure 1, is a four engine, delta wing, air refuelable medium bomber. It cruises subsonically but is capable of low altitude supersonic dashes up to Mach 2.0. It consists of the primary aircraft known as the "return component" and a "detachable pod" which has provisions for a special store and fuel. The combination of the "return component" and the "detachable pod" is referred to as the "composite aircraft." The fuselage is area-rule designed. The aircraft has a full cantilever midwing with a modified delta design and a conical cambered leading edge. All of the wing skin material is 248-T86. Panels 3, 5, 6 and 7 have aluminum honeycomb cores, all others have fiberglass honeycomb cores. Skin thicknesses are shown in Table 3.

The four General Electric engines equipped with after-burners are mounted on separate pylons attached to the underside of the wing. The aircrew consists of a pilot, navigator and a defense systems operator seated in tandem cockpits. Design weights and load factors are shown in Table 1.

T-618, T-621 FUSELAGE OUTER SKIN
 T-99, T-152 WING UPPER SURFACE OUTER SKIN
 T-102, T-170, T-176 WING LOWER SURFACE OUTER SKIN
 T-110 WING LEADING EDGE
 T-196, T-197 ELEVON INNER FLANGE LOWER SURFACE

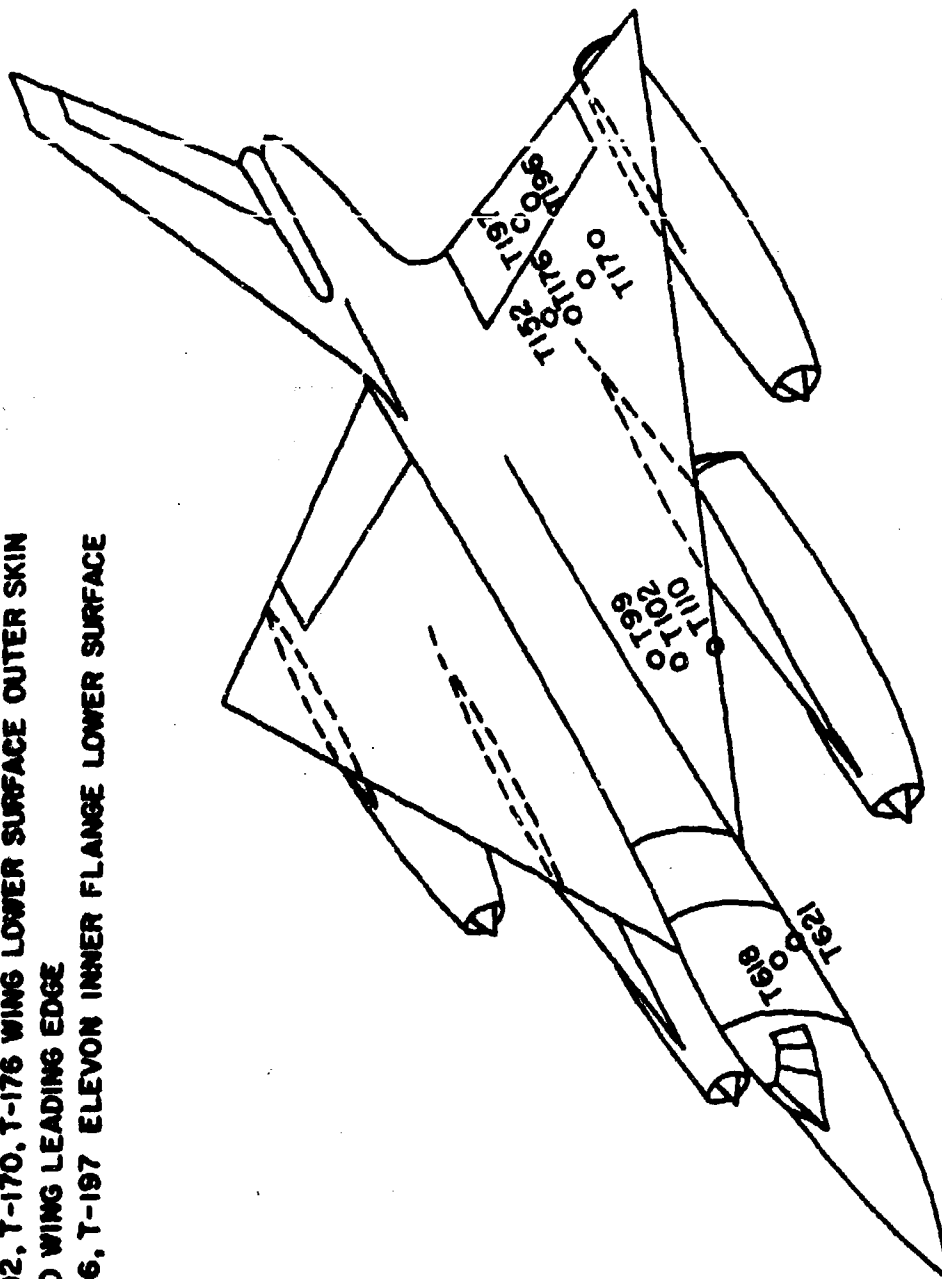


Figure 1. B-58A Aircraft with Thermocouple Locations

Table 1

Design Weights and Load Factors, B-58A

<u>Loading</u>	<u>Pounds</u>	<u>Design Limit Load Factor</u>	<u>Operational Limit</u>
Empty	55,000		
Basic	63,000		
Combat	100,000	+3.0, -1.0	+2.4, -0.8
Design	135,000	+2.0, 0.0	+1.6, 0.0
Max Take-Off	163,000		
Max In-Flight	176,845	+2.0, 0.0	+1.6, 0.0
Max Landing	95,000 (recommended)		

2.2.2 F-105D Aircraft Information

The F-105D aircraft, illustrated in Figure 2, is a single-place, air refuelable, supersonic, fighter-bomber. It is capable of attaining supersonic speeds at any operational altitude. The fuselage is an area-rule-design with swept back wings and empennage. Each wing incorporates an aileron and a spoiler. Each spoiler is made up of five sections designed to improve roll capabilities at high speed. The wing and fuselage skins are fabricated of 7075-T6 alclad aluminum alloy sheet. Temperature reduction procedures were used, where high engine temperatures were critical, such as, cooling air and insulation between the engine and structural components.

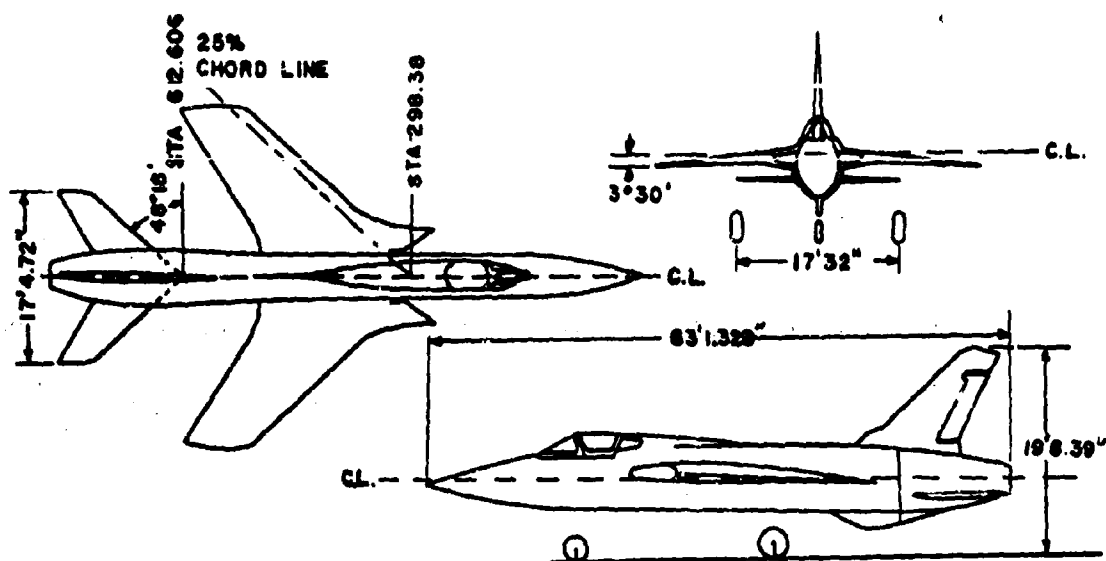


Figure 2. F-105D Aircraft

The power plant is a Pratt and Whitney J75-P-W turbojet engine equipped with an afterburner and water injection. Rated sea level static thrust of the uninstalled engine is approximately 16,100 pounds, with the afterburner 24,500 pounds and with the afterburner plus water injection 26,500 pounds.

The tricycle landing gear has a steerable nose wheel which can be engaged or disengaged by the pilot and automatically disengages after take-off. The primary flight controls are hydraulically actuated. Leading and trailing edge flaps are provided to increase lift, while a four section speed brake and drag chute are installed at the aft end of the fuselage to allow increased drag. Stores are carried in a fuselage

inclosed bomb bay, thereby keeping the aircraft aerodynamically clean, however, a variety of external stores increases its capabilities as a fighter-bomber. The F-105D is an 8.67" airplane subsonically and 7.33" airplane supersonically with no external stores and within certain weight and altitude limitations. It is capable of velocities up to Mach 2.1 at 35,000 to 50,000 feet altitudes (Reference 8). Table 2, below, lists the design weights and design load factors.

Table 2

Design Weights and Load Factors, F-105D

<u>Loading</u>	<u>Pounds</u>	<u>Load Factor</u>
Clean without bomb bay tank	35,200	8.67, 7.33, -3.0
Clean with full bomb bay tank	37,400	
Full bomb bay tank, 2-450 gal ext tanks	44,400	
Full bomb bay tank, 2-450 gal, 1-650 gal ext tanks	49,800	

2.3 Instrumentation

2.3.1 B-58A Aircraft Instrumentation

Flight test measurement schedules were categorized as follows for simplicity:

1. Temperature
2. Pressure
3. Position
4. Acceleration
5. Signals

The instrumentation was extensive in each of the above areas, for example, there were 400 temperature gages, 100 pressure gages, 15 position gages, 75 acceleration gages and 42 signal gages, however, not all of these gages were active during any single flight. The temperature gages were FeC (Iron Constantan) type thermocouples. Flight data were recorded on airborne Victor magnetic tape recording equipment. In order to conserve tape tracks, signals from up to 16 thermocouples were commutated. Due to the slowly varying nature of the thermocouple intelligence signal, rate of sampling was once every 9 seconds. The data were further condensed by multiplexing the outputs of two or more subcarrier oscillators and recording on one tape track. To increase data reliability, two reference thermocouples were sampled by each commutator.

The tapes were reduced on Victor playback units and the data presented versus time on Sanborn records. The Sanborn records were manually reduced and the temperatures tabulated.

Since this report is basically concerned with thermal measurements, only the locations of thermocouples are listed herein. Also, since thermal measurements were not critical, the contractor only listed the results of a sample number of gages and a sample section of two flights in their report (Reference 1). The location of these representative temperature gages is shown in Table 3 and in Figure 1 (References 2 and 3).

Table 3

Temperature Measurement Schedule, B-58A

<u>Gage Nr.</u>	<u>Test Item</u>	<u>Left Hand Wing Sta</u>	<u>Span Sta</u>	<u>Skin Gage</u>
T-99	Wing Outer Skin Upper Surface	198	42	.020
T-102	Wing Outer Skin Lower Surface	198	42	.020
T-110	Leading Edge Outer Skin	200.5	115	.020
T-152	Wing Outer Skin Upper Surface	509	131	.040
T-170	Wing Outer Skin Lower Surface	530	158.5	.040
T-176	Wing Outer Skin Lower Surface	509	131	.040
T-196	Elevon Inner Flange Lower Surface	575	167.5	.01
T-197	Elevon Inner Flange Lower Surface	545	146	.01
T-618	Fuselage Outer Skin Fuselage Station	340	135WL	.057
T-621	Fuselage Outer Skin Fuselage Station	385	110WL	.057

2.3.2 F-105D Aircraft Instrumentation

F-105D airplane, S/N 53-1155, was instrumented to record accelerations, shear, bending, torsion, position, rates, control forces and temperatures in preparation for the flight loads survey. The data were recorded on two Consolidated Electrodynamics Corporation oscillographs, one Ampex 800 FM/FM magnetic tape system and a photo recorder. A RAC 15 channel telemetering unit was employed to transmit pertinent structural information. Chromel-alumel type thermocouples were employed to measure temperatures. Laboratory tests indicated that the temperature measurements were accurate within $\pm 15^{\circ}\text{F}$.

Since this report is basically concerned with thermal measurements, only the locations of thermocouples are given. Also, since thermal measurements were not critical, the contractor only listed the results of a sample number of gages in his reports and data sheets. The location of these representative gages is shown in Table 7.

To measure the spar cap temperatures, thermocouples were installed .08 inches below the surface of the upper and lower spar caps respectively. These thermocouples were installed at wing station 145, fuselage station 483.7.

2.4 Description of Tests

2.4.1 B-58A Airplane Tests

The temperature loads survey tests were conducted by the Convair Division of General Dynamics Corporation. Table 4 below, shows the flight test requirements for the B-58A structural temperature survey (Reference 4). These tests were designed to provide critical stress and temperature data.

Table 4

Test Conditions, B-58A

<u>Data Run</u>	<u>Condition</u>	<u>Altitude</u>	<u>Mach Nr.</u>
1	Ground	-	-
2	Ground	-	-
3	T/O	-	-
4	T/O	-	-
5	Climb	-	-

<u>Data Run</u>	<u>Condition</u>	<u>Altitude</u>	<u>Mach Nr.</u>
6	Climb	-	-
7	Climb	-	-
8	Level	36,000	2.0
9	Level	36,000	2.0
10	As Required	Low	0.7
11	As Required	Low	1.2
12	Level	Maximum	0.95
13	Accelerate	Max/36,000	0.95/2.0
14	Decelerate	36,000/-	2.0/0.95
15	Max Speed	0/36,000	0/2.0

Tests were performed in both "return component" and "composite" configurations. Transient maneuvers were performed to 2.4"g" which was the operational limit for this aircraft (Section 2.2.1 and Table 1). Significant segments of the flight test profiles are shown in Figures 3 and 9. All test conditions were satisfactorily completed except that some deviations from the planned test profiles were necessary due to performance limitations of the J79-1 engines and to airframe restrictions (Section 2.2.1). Major deviations involved design speed flights which were performed at higher altitudes than planned and modified flight profiles for acceleration and deceleration maneuvers. Inspection of Figures 3 and 9 indicates that the desired Mach numbers were attained, however, the

altitudes were higher than planned (Table 4). As noted above there was an 80 percent design load factor restriction, however, these tests were effective in providing valid data which were useful in achieving the planned objectives.

2.4.2 F-105D Airplane Tests

The F-105D aircraft temperature loads survey was conducted by the Republic Aviation Corporation on airplane D-10, G/N58-1155. Five flight conditions were flown to obtain the most critical temperature conditions as shown in Table 5 below.

Table 5
Test Conditions, F-105D

<u>Flight</u>	<u>Condition</u>	<u>Altitude</u>	<u>Load Factor</u>	<u>Mach Nr.</u>
53	Max Power Accelerate to	40,000		2.0
54	Max Power Accelerate to	34,500		1.99
233	Max Power Accelerate to	40,000		2.07
21F-4	Max Design Load Factor	41,400	5.8	2.10
21F-5	Max Design Load Factor	28,000	7.6	1.56

The two high speed symmetrical pull-outs (flights 21F-4 and 21F-5) from banking turns were performed to limit load factor at 41,400 feet and 28,000 feet (Reference 9). Temperatures at these altitudes and at the time of the tests were -76°F and -13°F respectively. The first temperature was 6°F colder than the standard day and the latter temperature (-13°F) was 27°F warmer than the standard day temperature.

The symmetrical pull-out at 41,400 feet was performed subsequent to "heat soaking" the aircraft by accelerating to and maintaining a Mach number of 2.09 to 2.10 for 40 seconds. The pull-out was then executed at Mach 2.08 to 1.85 during a 15 second time interval and the maximum measured load factor was a 5.8"g" at a gross weight of 32,740 pounds. This gross weight was 4 percent lower than the design gross weight of 34,018 pounds (Figures 18 and 19).

The symmetrical pull-out at 28,000 feet was executed subsequent to "heat soaking" the structure by accelerating to and maintaining Mach numbers 2.09 to 2.10 for 40 seconds and then maintaining Mach numbers 2.08 to 1.74 for 85 seconds. The maximum load factor obtained was 7.6"g" at Mach number 1.56 and a gross weight of 31,600 pounds. This gross weight was 7 percent less than design (34,018) pounds.

2.5 Discussion of Data

2.5.1 B-58A Airplane Test Data

The bulk of the temperature data, which was used to determine whether any unknown critical temperature problem existed, is not included within this report since no critical temperature problems were revealed.

The B-58A temperature data shown herein were extracted from segments of two flights: numbers 37 and 48. These two flight profiles are shown in Figures 3 and 9 respectively. These figures indicate that the planned Mach numbers

were reached and marginally exceeded. The maximum planned Mach number was 2.0 (Table 4), whereas, the maximum recorded Mach number was 2.11 (Figure 9). The maximum attained altitude was 44,300 feet (Figure 3), which is greater than originally planned but is feasible as compared to the test plan (Table 4). Figures 3 and 9 present the adiabatic wall temperatures for flights 37 and 48 respectively. These adiabatic wall temperatures indicate the maximum theoretically possible skin and internal structural temperatures due to aerodynamic heating and as a function of time. However, during flight 37 the maximum adiabatic wall temperature (215°F) was exceeded in the outer skin leading edge at wing station 200.5 (Figure 7) and on the outer skin at fuselage station 340 LH, 135 WL (Figure 8). These recorded temperatures were 220°F and 223°F respectively. Obviously, the differences between the theoretical and recorded temperatures were not significant, since, they are within the range of possible instrumentation error. The adiabatic wall temperature profiles (Figures 3 and 9) were exceeded intermittently at the lower temperatures, however, this is not considered significant since the values were low and the variation not excessive. Generally, the adiabatic wall temperature profile is very similar to the recorded temperature data profile. Where there are significant differences the adiabatic wall temperature profiles are usually conservative.

Representative recorded temperature data samples, which resulted primarily from aerodynamic heating, are presented in Figures 4 through 8 and 10 through 15. These figures indicate the degree of correlation between measured and predicted temperatures and are shown to provide a basis for verifying predicted temperatures and their associated mathematical procedures (Appendix II). In general, the temperature data in these figures show that differences between measured and predicted values are within the range of uncertainty introduced by input and instrumentation errors. The major sources of error in the input data for the predicted values are in the thermal conductivity of the honeycomb panel and in the free stream air temperatures. Errors in the measured temperatures involve both the thermocouple installation, recording system and the data reduction system. A conservative estimate of the confidence limits of the measured and predicted data is $\pm 20^\circ$ Fahrenheit. In a few cases there is a difference between measured and predicted values beyond that attributed to instrumentation errors. For these instances, the predicted values are conservative.

The temperature data in Figures 4 through 8 are typical of temperature histories at transient conditions, while the data in Figures 10 through 15 show the effects of a more sustained or steady-state type of flight. For the flight profile segments shown in Figures 3 (transient condition) and

9 (steady-state condition), the Mach numbers and altitudes varied from 1.0 to 2.08; 1.9 to 2.11; 38,000 to 44,300 feet; 42,700 to 44,000 feet respectively. Generally, in a range where the Mach numbers were similar for both conditions (transient and steady-state), the temperatures were in good agreement, which indicates that Mach number and not flight condition (transient or steady-state) affects temperature. Where the Mach number varied, the temperatures varied in direct proportion, which is indicated by the following basic formulae for stagnation and adiabatic wall temperatures.

$$2.5.1.1 \quad T_{t0} = T_0 \left(1 + \frac{\gamma-1}{2} M^2 \right)$$

$$2.5.1.2 \quad T_{aw} = T_0 \left(1 + r \frac{\gamma-1}{2} M^2 \right)$$

The majority of the recorded data as shown in Figures 4 through 8 and 10 through 15 was less than 180° Fahrenheit. The highest temperatures (above 200°F) were recorded at the wing leading edge, wing station 200, span station 115; fuselage outer skin station 310LH, 135WL; wing station 509, span station 131; and eleven wing station 545, span station 146. The highest recorded temperature was 223°F at fuselage station 340 LH, 135WL which is 8°F higher than the maximum adiabatic wall temperature for this flight condition. It is observed that temperatures above 200°F were recorded on the wing leading edge and aft portion of wing.

Figure 16 portrays fuselage station 340 LH, 135 WL temperatures versus Mach number. These data are plotted here because maximum temperatures (maximum temperature 223°F) were registered at this fuselage station, and to show that temperature is a function of Mach number. The circles (O) are measured data plots during flight path acceleration. The triangles (Δ) are data plots during deceleration from the peak Mach number (2.08). The deceleration temperatures for any given Mach number are higher (10° to 40°F) than the acceleration temperatures. This indicates a temperature lag in the fuselage skin. The diagonal line AB is drawn through the maximum accelerated flight temperatures to show a maximum possible temperature for any given Mach number. The equation for this line is:

$$T = 192.5M - 175$$

This equation will be tested as more data becomes available.

Figure 17 shows wing leading edge station 200 temperatures versus Mach number. These data are plotted because maximum wing temperatures (maximum temperature 220°F) were registered at this wing station, and to further indicate that temperature is a function of Mach number. The circles (O) are measured data plots during flight path acceleration. The triangles (Δ) are data plots during deceleration from peak Mach number (2.08). The deceleration temperatures for any given Mach number are generally higher (5°-20°F) than the acceleration temperatures. This indicates a temperature lag in the wing leading edge

skin, but to a lesser degree than in the fuselage skin (Figure 16). This is attributed to the thinner skin (.020") in the wing leading edge as opposed to a skin thickness of .057" in the fuselage skin. The data in Figure 17 show nearly a straight line relationship from Mach 1.0 to 2.0, after which, the temperature appears to build up more rapidly. This condition will be checked as more data become available. The diagonal line CD is drawn through the maximum accelerated flight temperatures to show a maximum possible temperature for any given Mach number. The equation for this line is:

$$T = 225M - 250$$

The lines AB and CD in Figures 16 and 17 show considerable deviation at Mach 1.1 but as Mach number increases, the deviation decreases until it appears the lines would intersect at about Mach 2.12, thus indicating identical temperatures at this velocity.

Figures 16 and 17 show data from flight 37 only. The Mach number range for flight 48 was not sufficient to show any significant profiles.

In summary, it appears that the recorded temperature data were reliable and correlated quite well with predicted temperature values. Although all design conditions could not be attained due to engine performance limitations and airframe restrictions, it is reasonable to assume that the temperature data will also correlate well at design conditions which were now flown. Also, the recorded temperatures were not excessive for the aluminum alloy wing skin (248-T86).

The calculated and measured nacelle former temperatures, which are shown in Table 6, are higher than the temperatures shown in Figures 4 through 8 and 10 through 15, because the nacelle former temperatures resulted primarily from engine heating. These temperatures are functions of speed, altitude and engine power setting. The calculated temperatures were computed by solving the steady-state heat balance equations for two representative steady-state conditions, also shown in Table 6. Condition I, as seen in Table 6 is the more critical condition, however, the predicted and measured temperatures are in good agreement, the overall average difference being less than 5%. Also, the predicted values are conservative. In conclusion, the steady-state heat balance equations (Appendix II) served very well for predicting engine induced structural temperatures at Mach 2.05.

Condition II (Table 6), where the Mach number is only 0.935, shows poor and intermittent correlation between the predicted and measured temperature data. This may indicate that the steady-state equations may not be appropriate for low Mach numbers, however, this low Mach number flight condition does not constitute a temperature problem, therefore, further discussion is unnecessary.

Table 6
Predicted and Measured Nacelle Former
Temperatures, B-58A

Nacelle Station	Flange	Condition I		Condition II	
		Predicted	Measured	Predicted	Measured
125	inner	246°F	234°F	+14°F	+1°F
125	outer	231°F	219°F	+ 7°F	-7°F
227	inner	567°F	512°F	300°F	287°F
227	outer	412°F	412°F	136°F	174°F
244	inner	550°F	510°F	288°F	293°F
244	outer	414°F	408°F	132°F	183°F

	Condition I	Condition II
Mach Number	2.05	0.935
Pressure Altitude	43,000'	30,000'
Adiabatic Wall Temperature	213°F	-5°F

2.5.2 F-105D Airplane Test Data

The bulk of the temperature data, which was used to determine the existence of any unknown critical temperature condition, is not included within this report since no critical temperature problems were revealed.

Representative temperature data are shown in Table 7 with their corresponding design temperatures (References 6 and 7) as available. The design limit values, where available, exceed

the measured values by a rather significant margin. Methods using the heat balance equations for calculating design temperatures are shown in Appendix III and Reference 6.

The most severe temperature condition was in flight 21F-4 (Table 5) where the Mach number was 2.10 and the altitude 41,400 feet. For this condition, the free stream total temperature is 274°F and the corresponding adiabatic wall temperature is 240°F . Accordingly, 274°F is the maximum theoretical temperature for ram ventilated compartments and 240°F is the maximum theoretical temperature for aircraft surface elements which are subjected to aerodynamic heating. The 240°F surface temperature is 23°F or about 10 percent higher than the maximum recorded surface temperature of 217°F at fuselage station 734 (Table 7). The F-105D airplane was designed to an adiabatic wall temperature of 240°F and a stagnation temperature of 250°F (Reference 5). These latter temperatures were based on flight at Mach 2.06 and 34,000 feet altitude. Application of this design speed and altitude to the basic formulae for calculating adiabatic wall temperature and stagnation temperature gives 235°F and 269°F respectively. The contractor (Reference 5) did not assume an absolute free stream temperature but modified it by assuming a 0.3 Mach number for air velocity in the ducts. This was to conform to the 250°F free stream temperature which was used in the design

of the F-105B airplane. However, this temperature (250°F) was based on a Mach number of 2.0 at 35,000 feet altitude. It is apparent from Table 7 that the F-105B measured temperatures were significantly less than the design temperatures, the two predicted temperatures are not critical for aluminum at the most severe flight conditions that were flown. It is observed in Table 7 that the last three temperatures, which resulted from engine heating, are significantly higher than the preceding measured temperatures, however, they are less than design temperatures.

Table 7

Flight Test Temperature Data, F-105D

Item	Fuselage Station	Max. Temp °F		Alt.	Condition
		Design Limit	Measured		
Frame inner flange	734	300	217	40,000'	at Mach 2.0
Drag chute floor	710	270	127	40,000'	at Mach 2.0
Upper L/H frame	633	311	140	34,500'	at Mach 1.99
Upper R/H frame	633		115	34,500'	at Mach 1.99
Lower R/H frame	633		122	34,500'	at Mach 1.99
Upper R/H frame	635	385	175	34,500'	at Mach 1.99
Lower R/H frame	635	385	162	34,500'	at Mach 1.99
Cell 3D Floor	575	280	111	34,500'	at Mach 1.99
Fuselage skin inner surface	610	225	183	34,500'	at Mach 1.99
Frame inner flange, top	576	270	145	34,500'	at Mach 1.99
Frame inner flange, side	576		180	34,500'	at Mach 1.99
Airframe engine mt. lower L/H	501		91	34,500'	at Mach 1.99
Airframe engine mt. upper L/H	501		91	34,500'	at Mach 1.99
Horizontal stabilator beam	688		120	34,500'	at Mach 1.99
Bottom cell 3D	610		75	40,000'	at Mach 2.07
Leading edge flap - wing sta	145		195	28,000'	at Mach 1.56
Leading edge flap - wing sta	145	201*		28,000'	at Mach 1.7
Leading edge flap - wing sta	145	229*	200	41,400'	at Mach 2.08
Upper spar cap - wing sta	145		120	41,400'	at Mach 2.08
Lower spar cap - wing sta	145		160	41,400'	at Mach 2.08
Active renewal case temp	716	725	430	40,000'	at Mach 2.07
Bath tub air temp	716		410	40,000'	at Mach 2.07
Cooling air temp	720	370	345	40,000'	at Mach 2.07

*Predicted temperatures

Figures 18 through 21 present temperature measurements from two maneuvers as discussed in Section 2.4.2. Before these maneuvers were performed, the aircraft was "heat soaked" at Mach numbers 2.09 to 2.10 for 40 seconds. The wing temperatures were all taken at wing station 145 on the upper and lower spar cap and on the flap leading edge inner skin. These figures show progressively increased temperatures from the upper spar cap to lower spar cap to flap leading edge inner skin. The lower temperatures on the spar caps are due to the gage location (Section 2.3.2) and also the large mass to be heated.

The data in Figures 18 and 19 were measured at an altitude of 41,400 feet. The maximum temperatures measured were: leading edge flap 200°F, top forward spar cap 120°F, lower forward spar cap 160°F. The predicted temperature on the leading edge flap for this condition was calculated to be 229°F after adjustment for the cold day at this altitude. At this time and altitude it was 6°F colder than the standard day temperature.

The data in Figures 20 and 21 were measured at an altitude of 28,000 feet. The maximum measured temperatures were: leading edge flap 195°F, top forward spar cap 120°F, bottom forward spar cap 140°F. During the test period at 28,000 feet, it was 27°F warmer than a standard day. The predicted leading edge temperature for this "hot day" condition and at Mach 1.7 is 201° Fahrenheit.

The measured temperatures for these two design flight conditions were lower than design and predicted values indicating that no aerodynamic heating temperature problems exist for the aluminum skin and spar caps at these Mach numbers and altitudes.

The measured nose boom temperatures shown in Figures 18 and 19 were compared with calculated values using the free stream total temperature formula and the "cold day" temperature:

$$T_{to} = T_o (1 + .2M^2)$$

There was good agreement as observed in Table 8. These differences range from 1 1/2 to 4 1/2 percent and are within instrumentation inaccuracies. Also, these measured temperatures indicate a slight lag in the temperature gages.

Table 8

Free Stream Total Temperature, Flight 21F-4, F-105D

Mach Number	Calculated °F	Δ °F	Measured °F	Δ °F
2.08	256	3	245	0
2.07	253	4	245	5
2.06	249	24	240	10
1.98	225	15	230	12
1.93	210	15	218	20
1.68	195	8	198	8
1.85	187		190	

The measured nose boom temperatures shown in Figures 20 and 21 were compared with calculated values using the free stream total temperature formula and the "hot day" temperature. Agreement was not as good as noted in Table 8 above. It would appear from the above figures and Table 9, below, that the first measured temperature (230°F) was in error and that there was a temperature lag down to the Mach 1.59 condition and following that, the drop was excessive. This could be due to temperature gage inaccuracies. The free stream total temperature formula appears to be reasonable.

Table 9

Free Stream Total Temperatures, Flight 21F-5, F-105D

Mach Number	Calculated °F	Δ °F	Measured °F	Δ °F
1.76	264	-6	230	+10
1.74	258	-6	240	-3
1.72	252	-6	237	-5
1.7	246	-18	232	-7
1.64	228	-15	225	-13
1.59	213	-14	212	-20
1.54	199	-13	192	-9
1.49	186	-3	183	-3
1.48	183	-13	180	-22
1.43	170	-8	158	-18
1.4	162	-12	140	-9
1.35	150		131	

In conclusion it is to be noted that measured temperatures on the F-105D aircraft were significantly less than design and predicted values and were not critical for aluminum alloy skin and spar caps. Also, nose boom measured temperatures generally agree with calculated values.

SECTION III

CONCLUSIONS

1. Measured temperatures were generally less than design or predicted. Some exceedances did occur, however, they were not excessive and no temperature problems were revealed by these tests.
2. The adiabatic wall temperature profile generally and conservatively defines the measured temperature profile.
3. Since B-58 aircraft measured temperatures were in agreement with predicted temperatures, temperature prediction techniques were considered satisfactory up to the maximum recorded Mach number (2.11).
4. Where similar Mach numbers existed, the B-58A aircraft measured temperatures from transient and steady-state conditions were in good agreement.
5. Steady-state heat balance equations served very well in predicting B-58A aircraft engine induced structural temperatures at Mach 2.05.
6. The highest measured temperature, resulting from aerodynamic heating, on the B-58A aircraft was 223°F at fuselage station 340LE, 135 WL.
7. The highest measured temperature from aerodynamic heating on the F-105D aircraft was 217°F at fuselage station 734. This shows good agreement with the B-58A aircraft's maximum measured

temperature (223°F). Their respective Mach numbers and altitudes were relatively close (Figure 3 and Table 7).

8. F-105D design temperatures were considerably higher than the measured temperatures.

9. Nose boom measured atmospheric temperatures were in fair agreement with calculated values using the free stream total temperature formula.

10. Measured atmospheric temperatures at altitude are not always in conformity with standard day temperatures.

REFERENCES

1. Convair Report FZS-4-203, dated 18 April 1960, "B-58A Structural Temperature Flight Survey"
2. Convair Report FZM-4-504, dated 1 May 1957, "Flight Test Instrumentation Report"
3. Convair Report FZM-4-504, Addendum 2, dated 1 July 1958, "Flight Test Instrumentation Report"
4. Convair Report FZS-4-164, dated 21 May 1958, "Structural Temperature Survey Requirements for B-58"
5. Republic Aviation Report DR 79-23, dated July 1959, "Stress Analysis Criteria-Temperature Criteria F-105D Airplane"
6. Republic Aviation Report EP 212, dated 11 September 1957, "Structural Temperature Analysis F-105B"
7. Republic Aviation Report ETR-11, dated 17 June 1959, "Structural Temperature Report F-105D"
8. Technical Order 1F-105D-1, dated 30 October 1963, "Flight Manual"
9. Republic Aviation Report EPTMR 4596, dated 12 October 1961, "Wing, Fuselage, Horizontal Tail Loads, Leading Edge Flap and Wing Temperatures Measured During Two High Speed Limit Load Factor Normal Symmetrical Pullouts on the F-105D (D-10) AF S/N 58-1155 Flight Loads Airplane"
10. Republic Aviation Corporation Report EFIIM-105-13, dated 20 July 1961, "Instrumentation Instruction Manual F-105D Aircraft S/N 58-1155 (D-10) Structural Integrity Testing"

APPENDIXES

APPENDIX I
Flight Profiles

Appendix I consists of flight profiles of Mach number, altitude, adiabatic wall temperature, measured and predicted fuselage, wing, tail and nose boom temperatures.

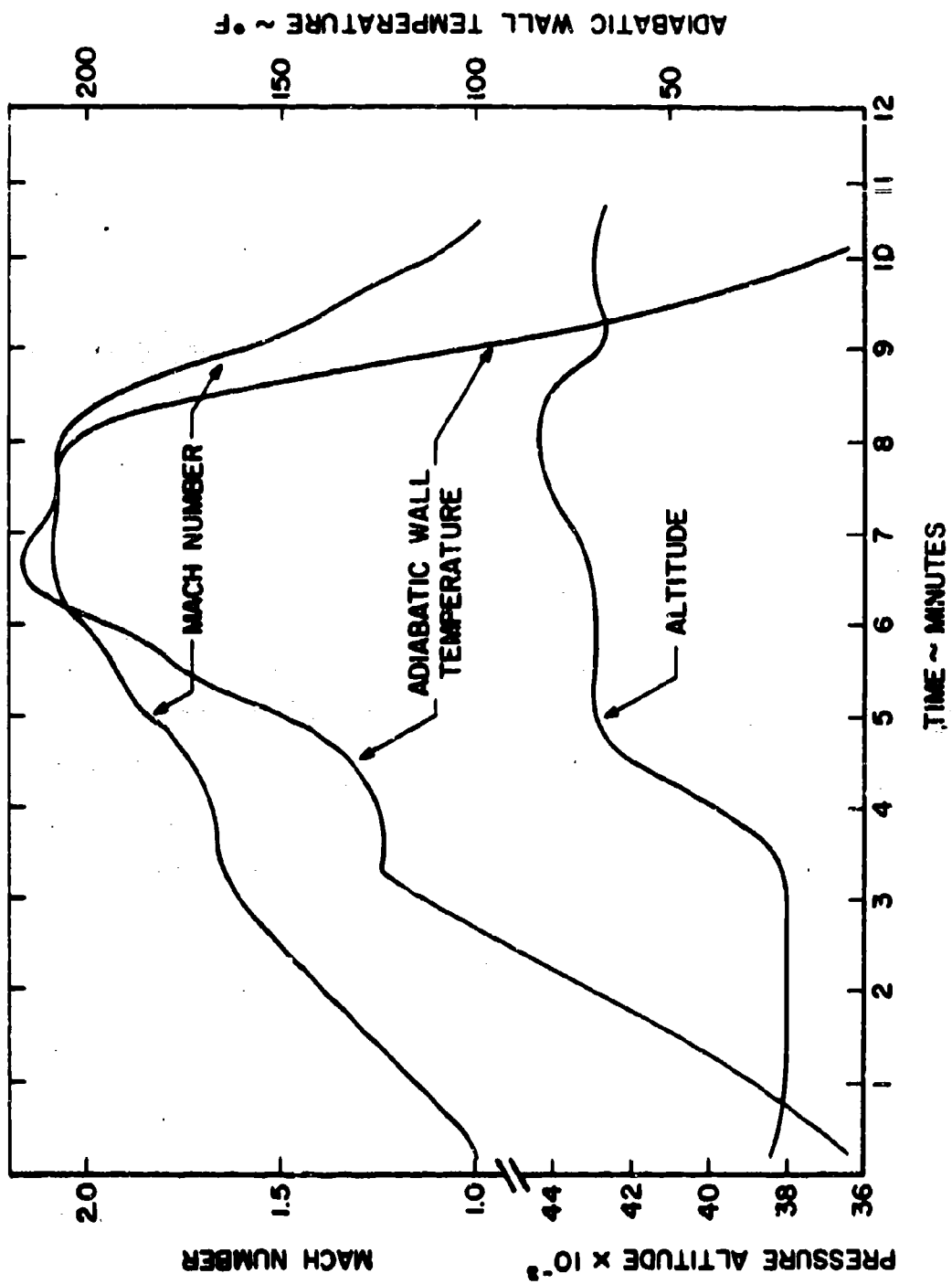


Figure 3. Flight Nr. 37 Profile, B-58A

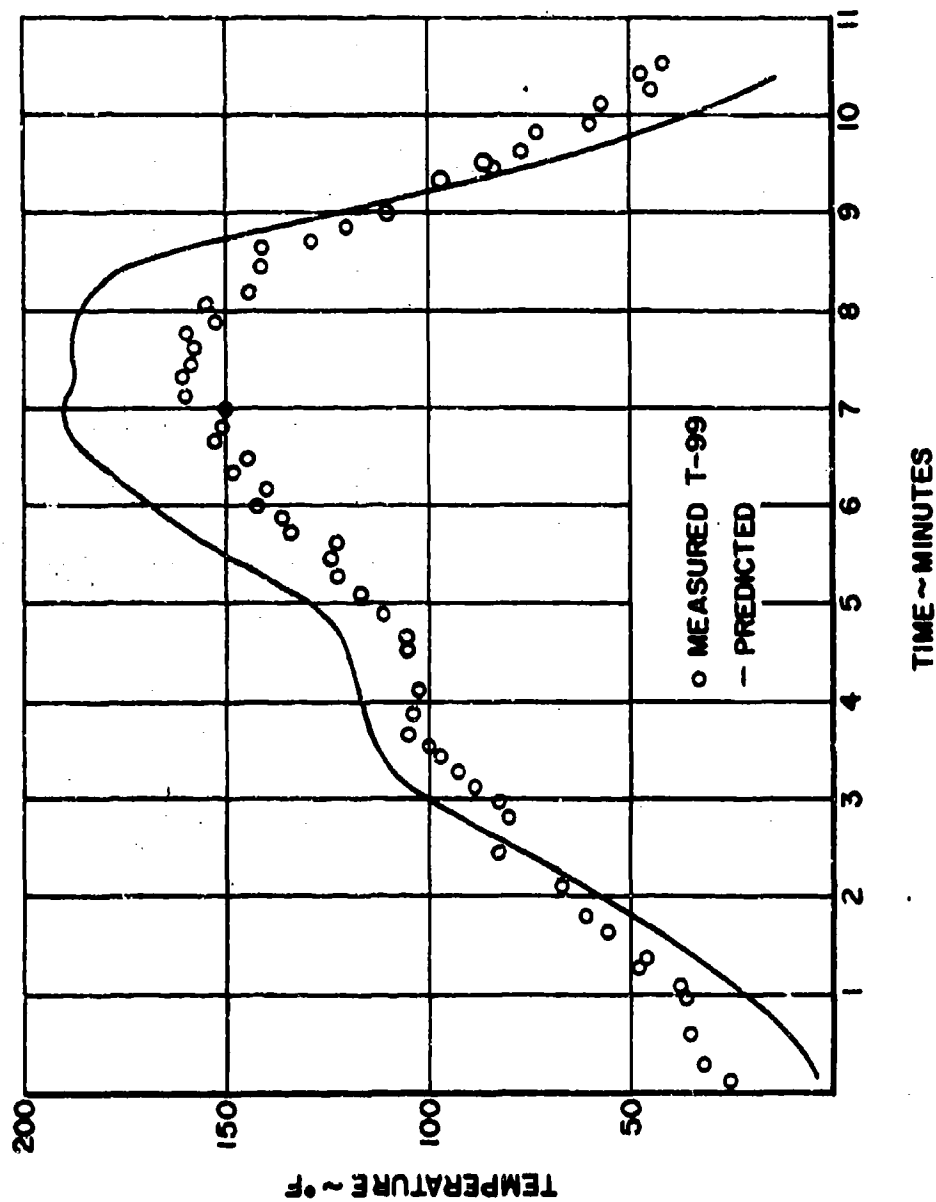


Figure 4. Wing Station 198 Upper Surface Outer Skin Temperature, Flight 37, I-58A

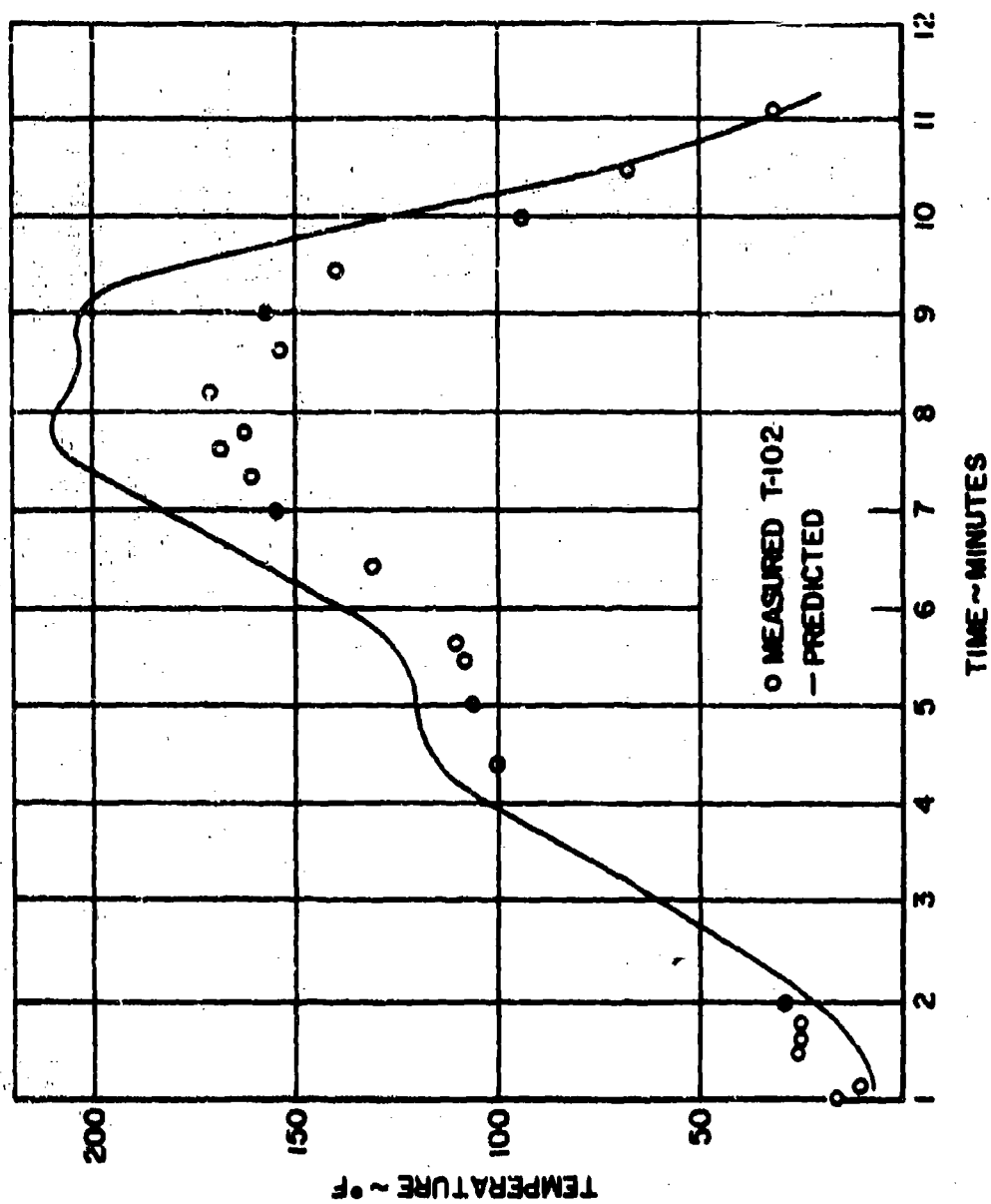


Figure 5. Wing Station 198 Lower Surface Outer Skin Temperature, Flight 37, B-58A

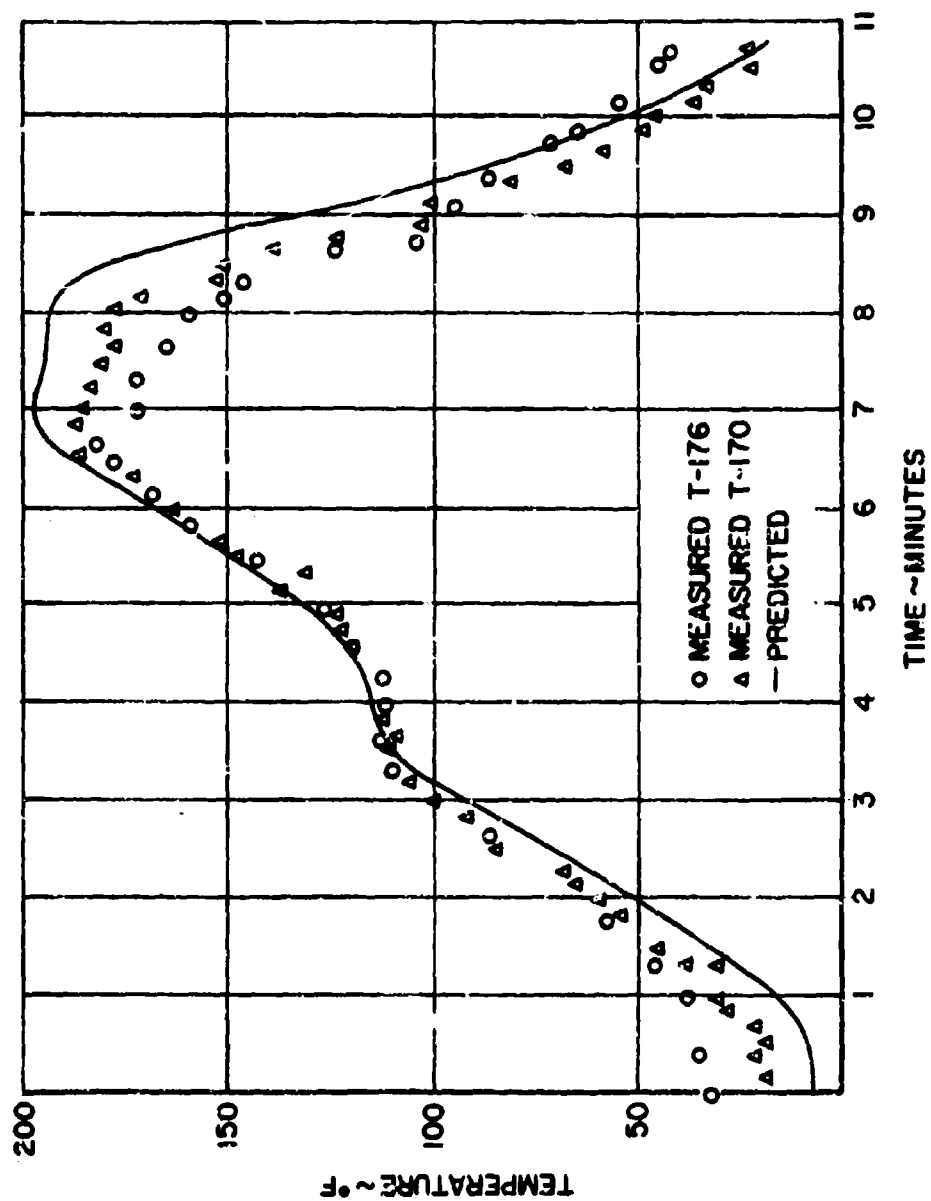


Figure 6. Wing Stations 509, 530 Lower Surface Outer Skin Temperature, Flight 37, B-58A

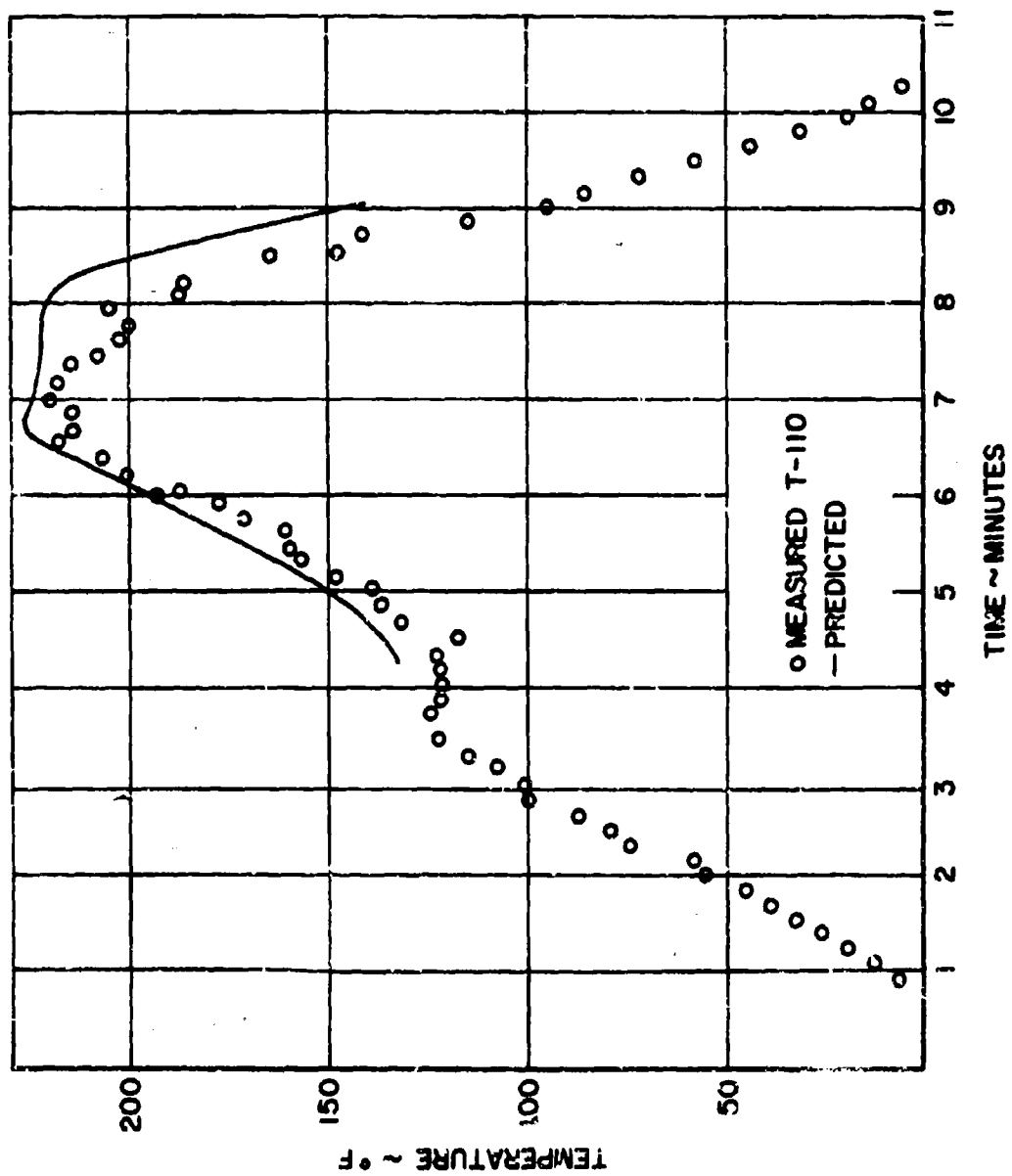


Figure 7. Wing Station 200 Leading Edge Temperature, Flight 37, B-58A

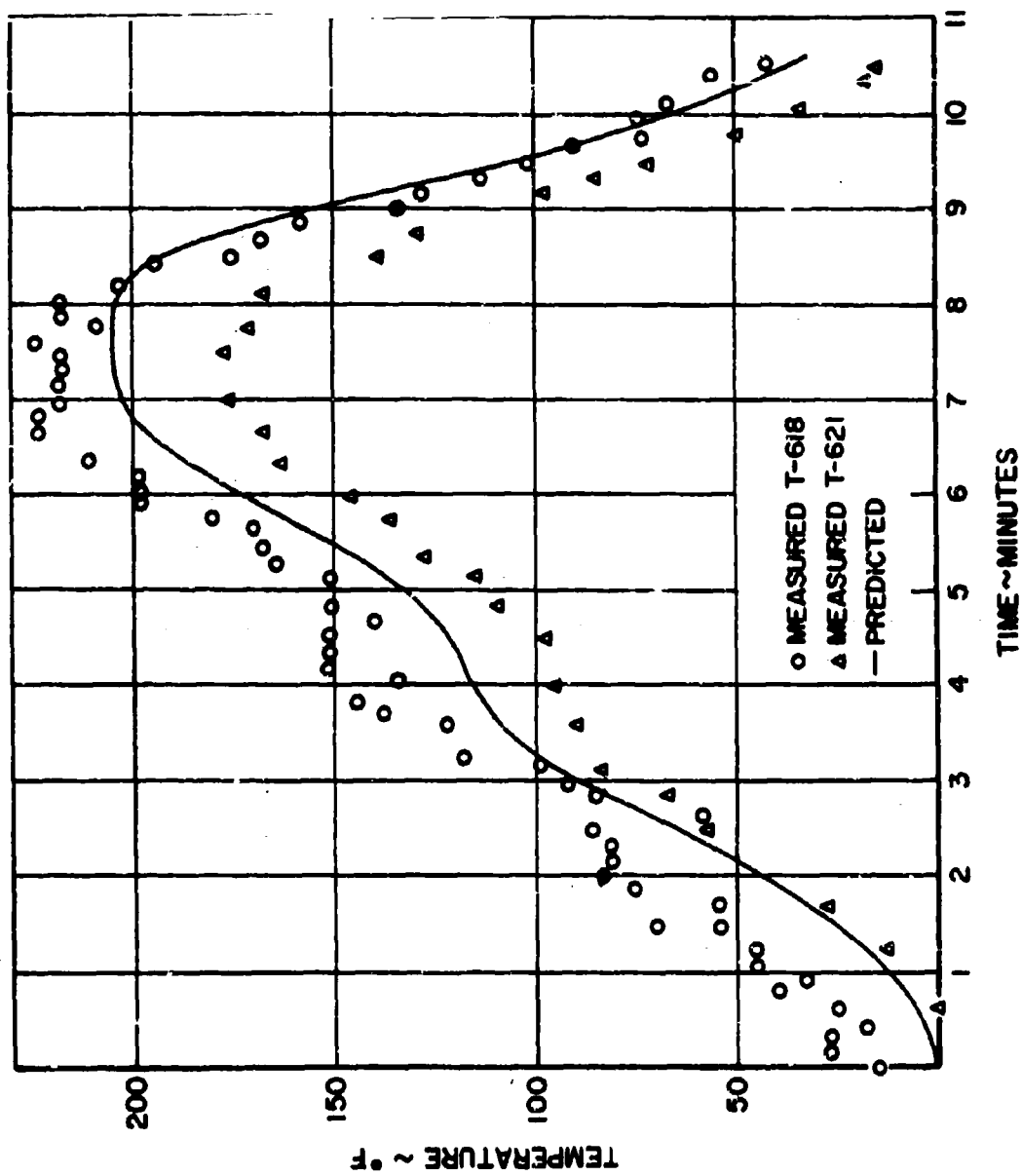


Figure 8. Fuselage Stations 340, 385 Skin Temperature, Flight 27, B-58A

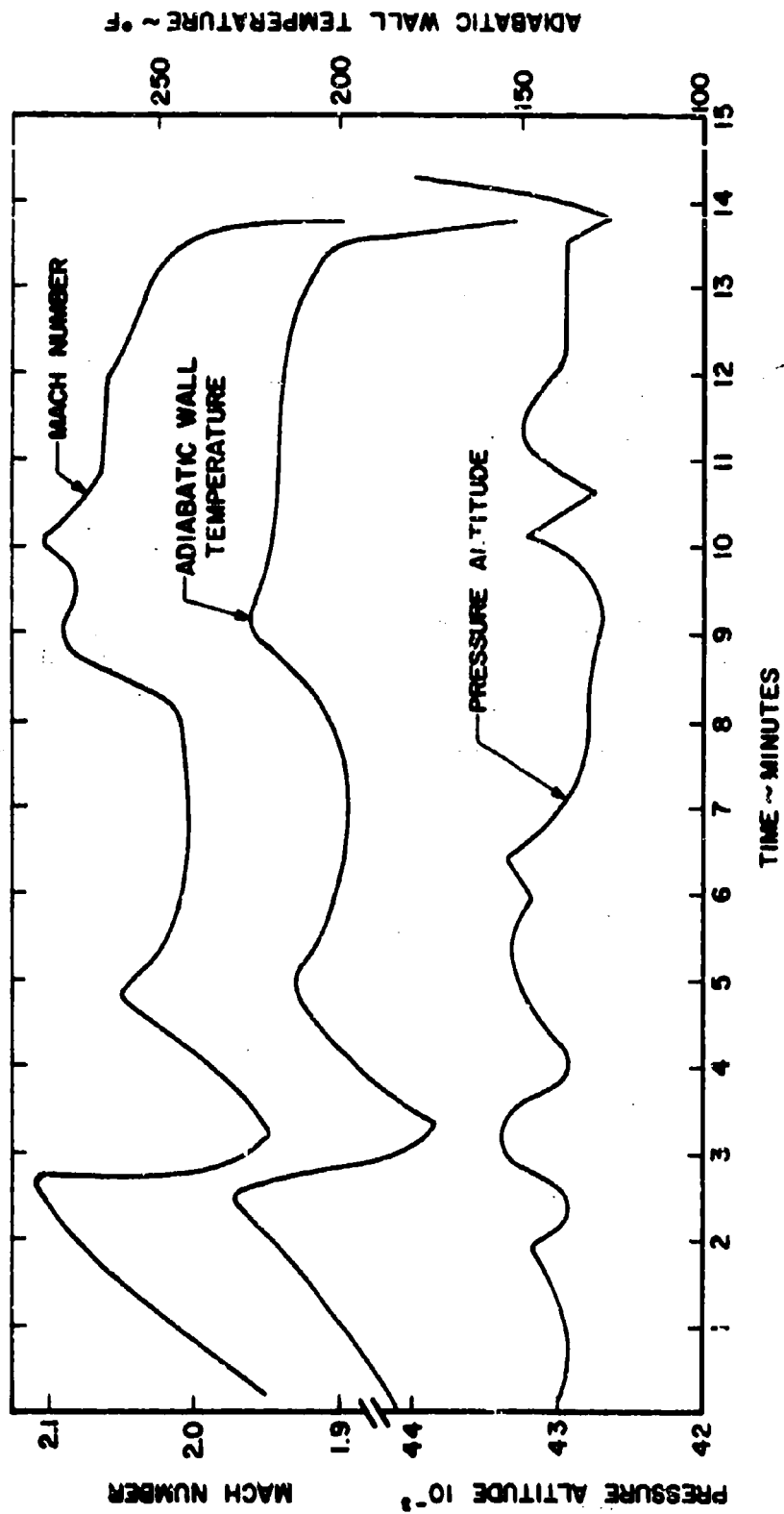


Figure 9. Flight Nr. 40 Profile, B-58A

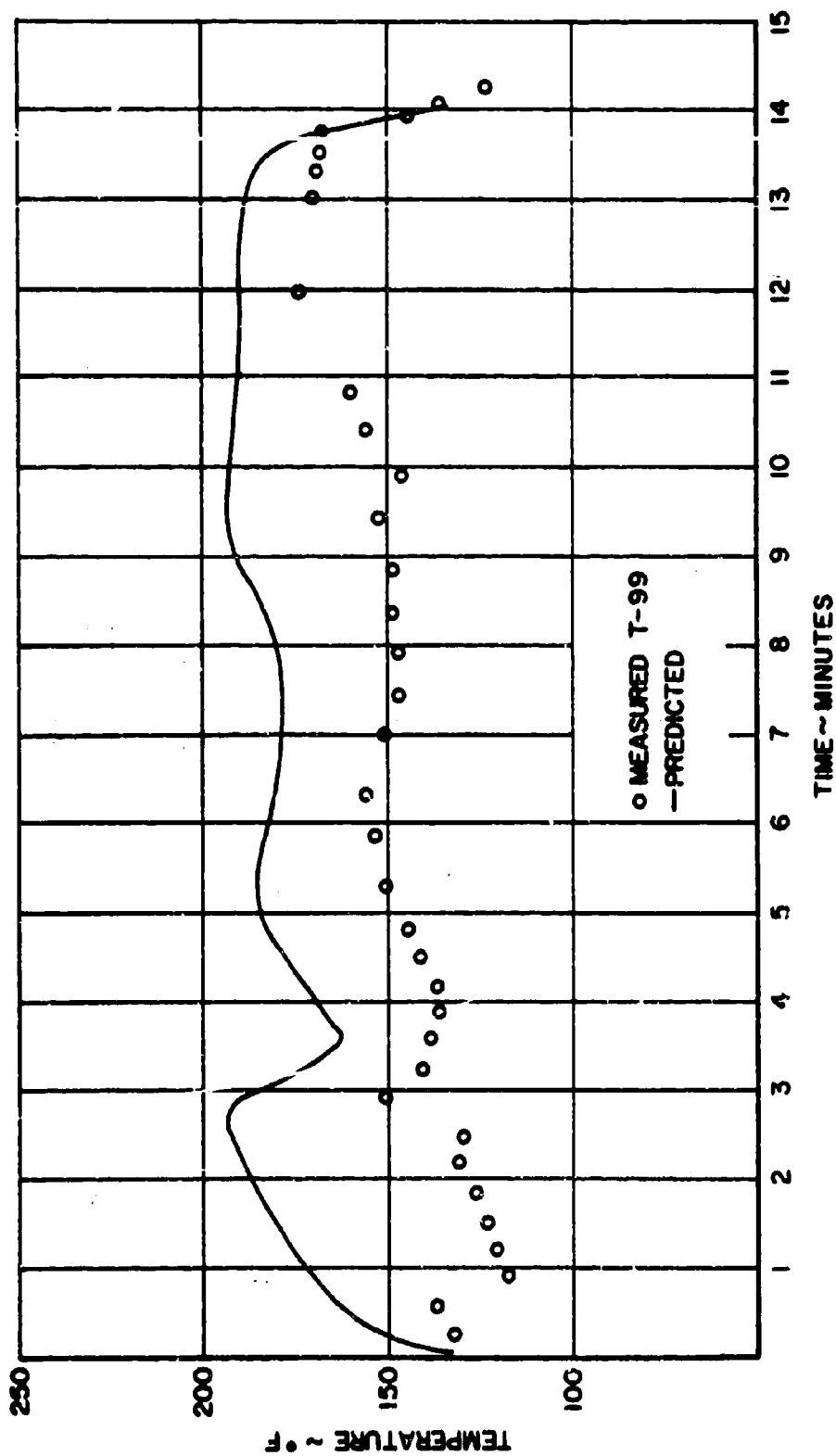


Figure 10. Wing Station 138 Upper Surface Outer Skin Temperature, Flight 48, B-58A

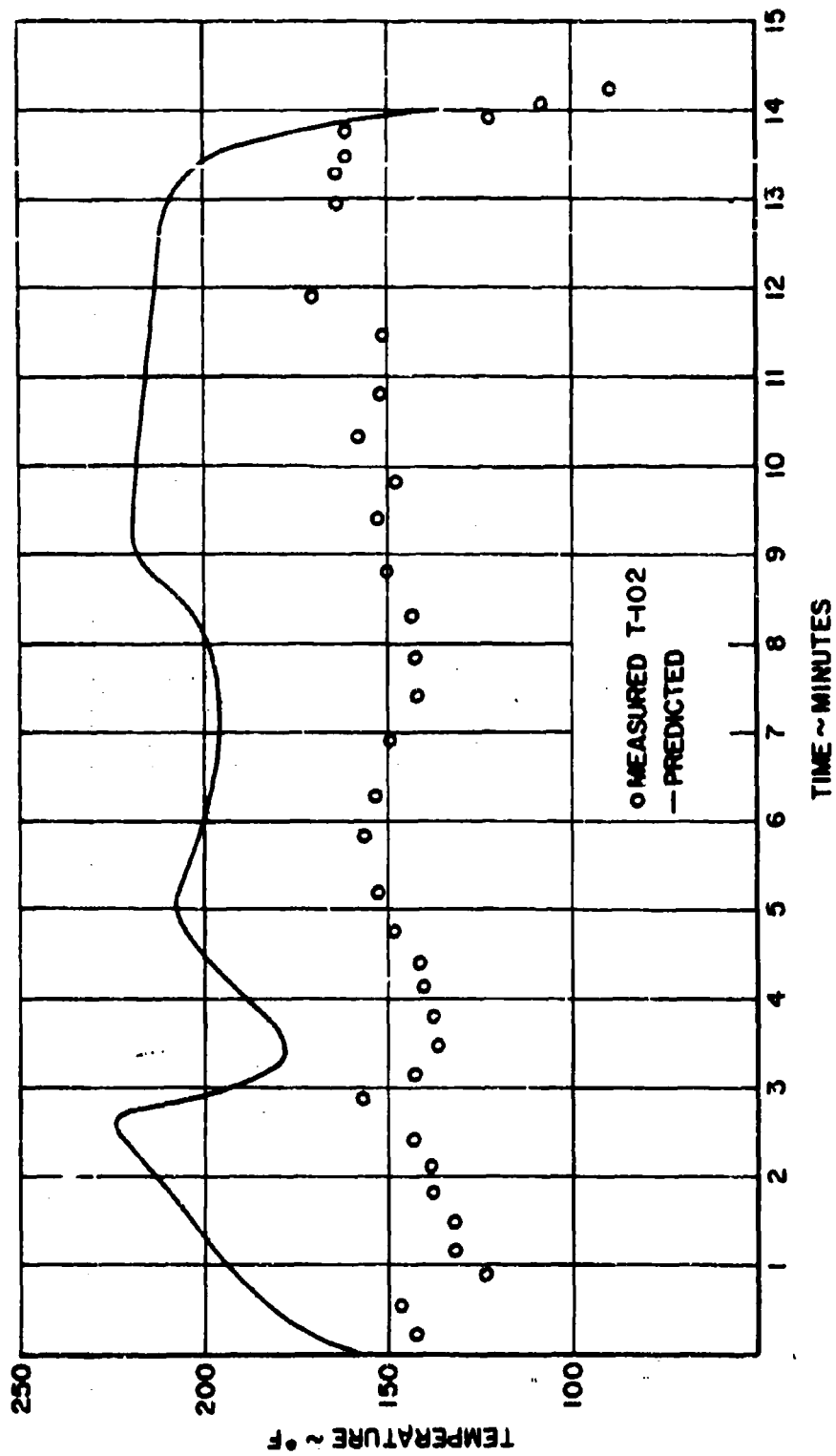


Figure 11. Wing Station 198 Lower Surface Outer Skin Temperature, Flight 48, B-58A

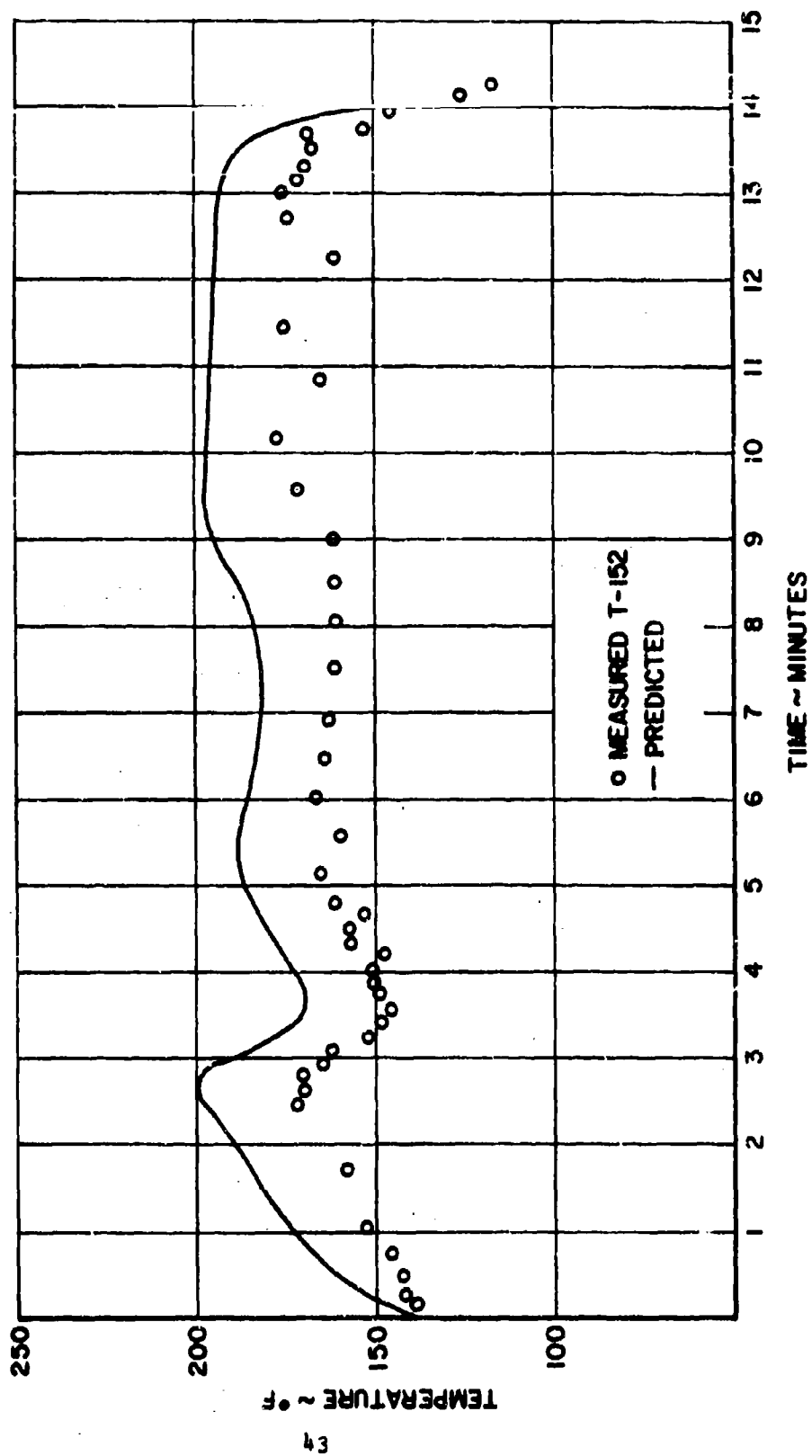


Figure 12. Wing Station 509 Upper Surface Outer Skin Temperature, Flight 48, B-58A

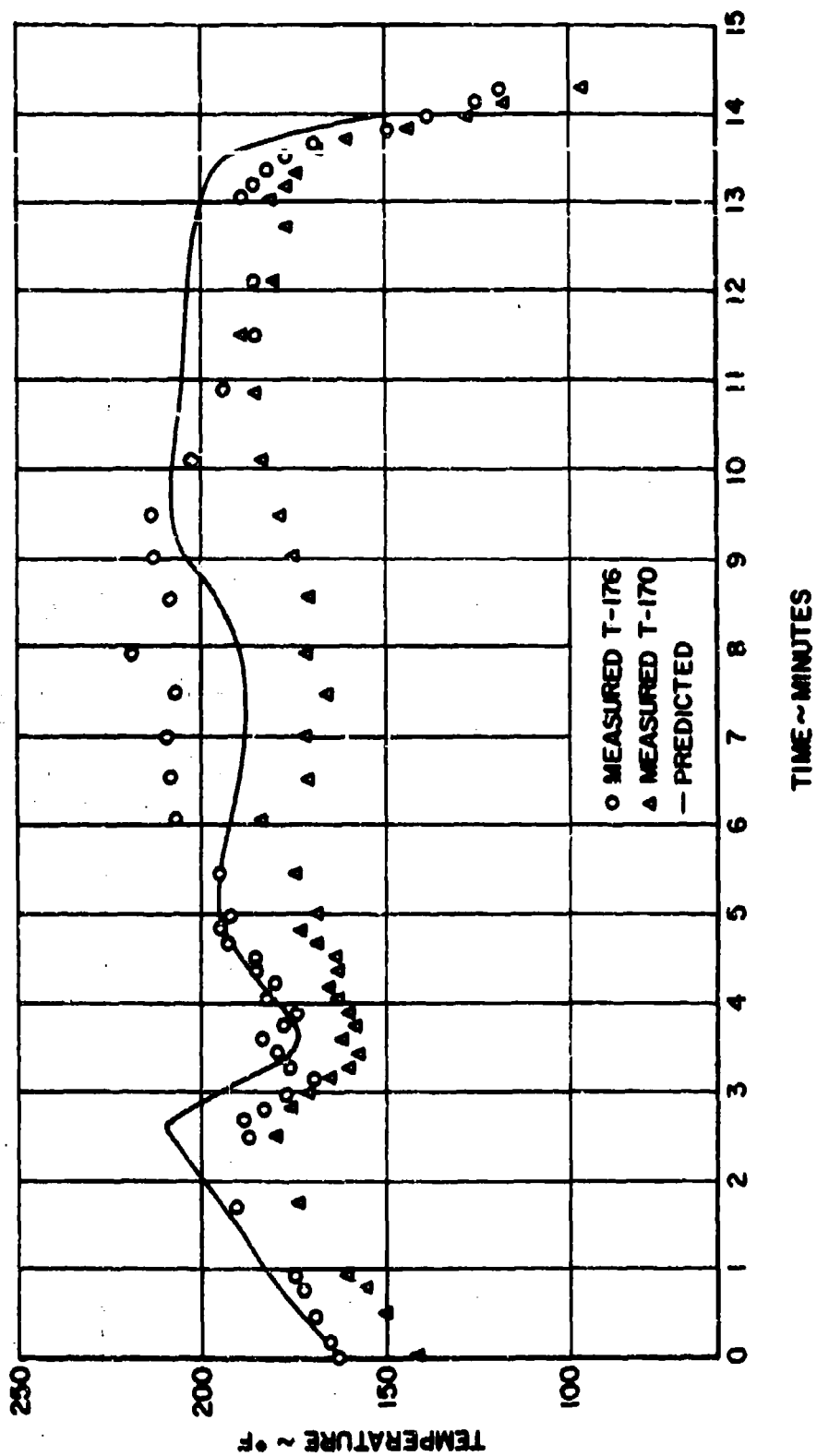


Figure 13. Wing Stations 509, 530 Lower Surface Outer Skin Temperature, Flight 48, B-58A

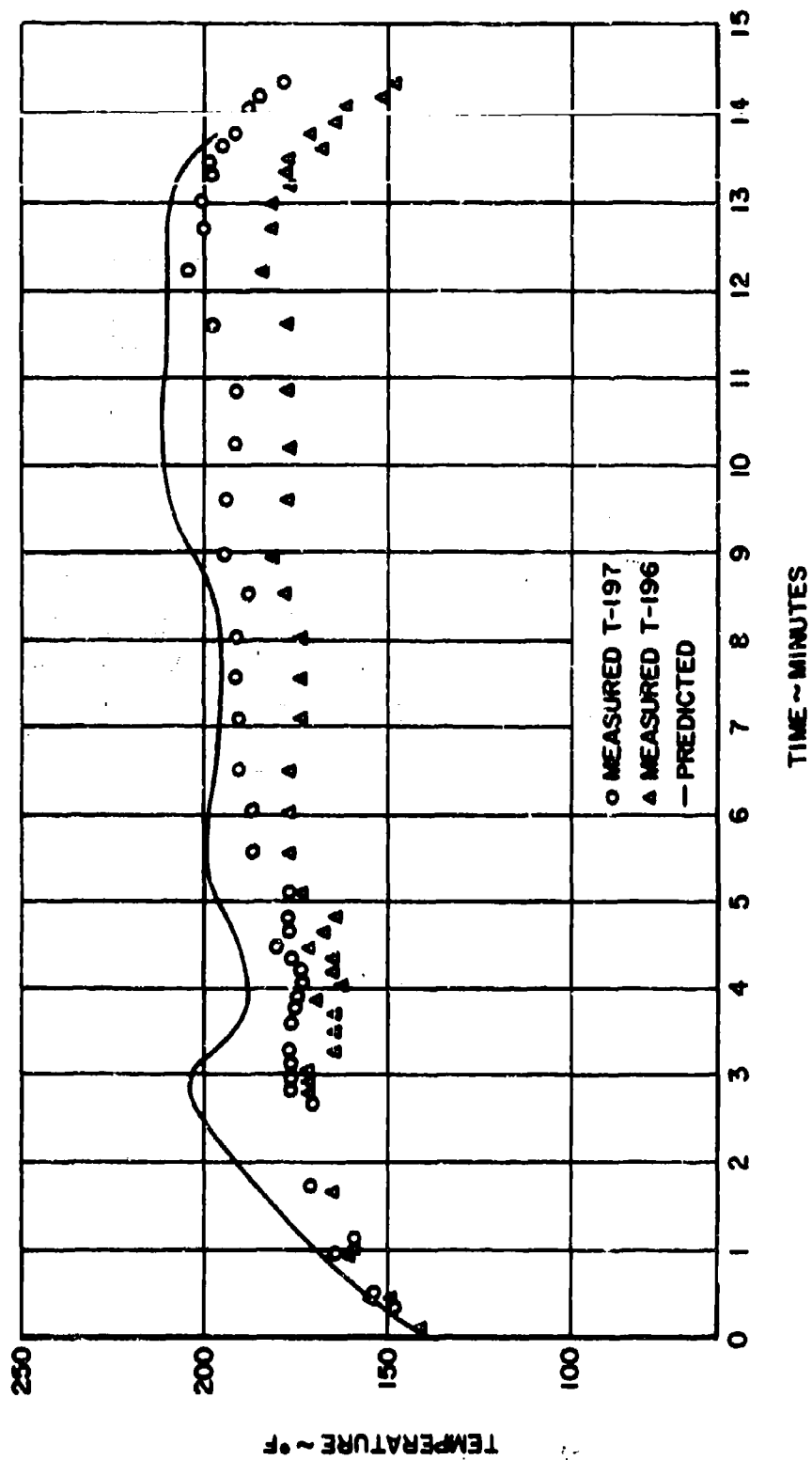


Figure 14. Elevon Inner Flange Lower Surface Temperature, Wing Stations 545, 575, Flight 48, B-58A

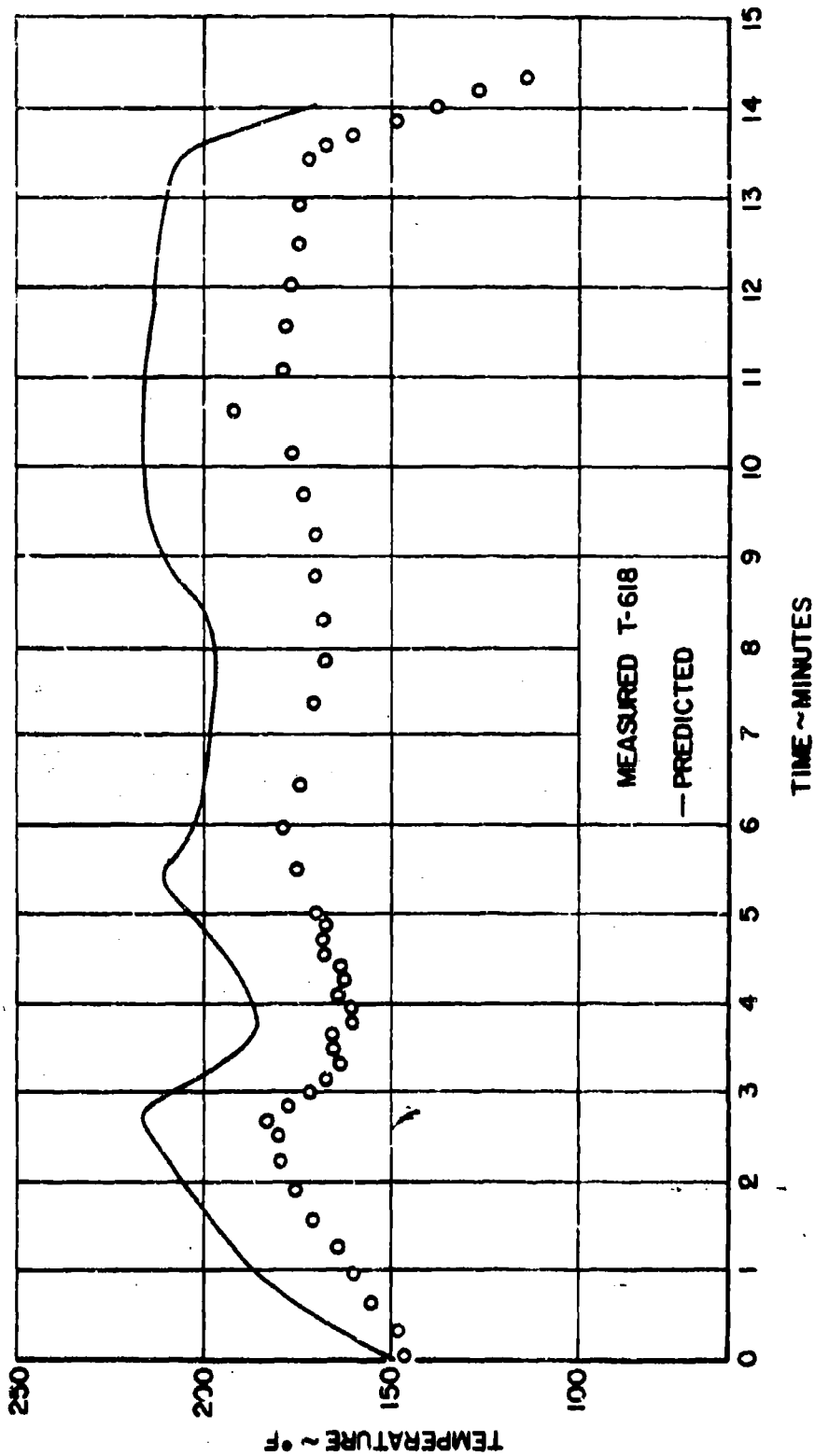


Figure 15. Fuselage Station 340 Skin Temperature, Flight 48, B-58A

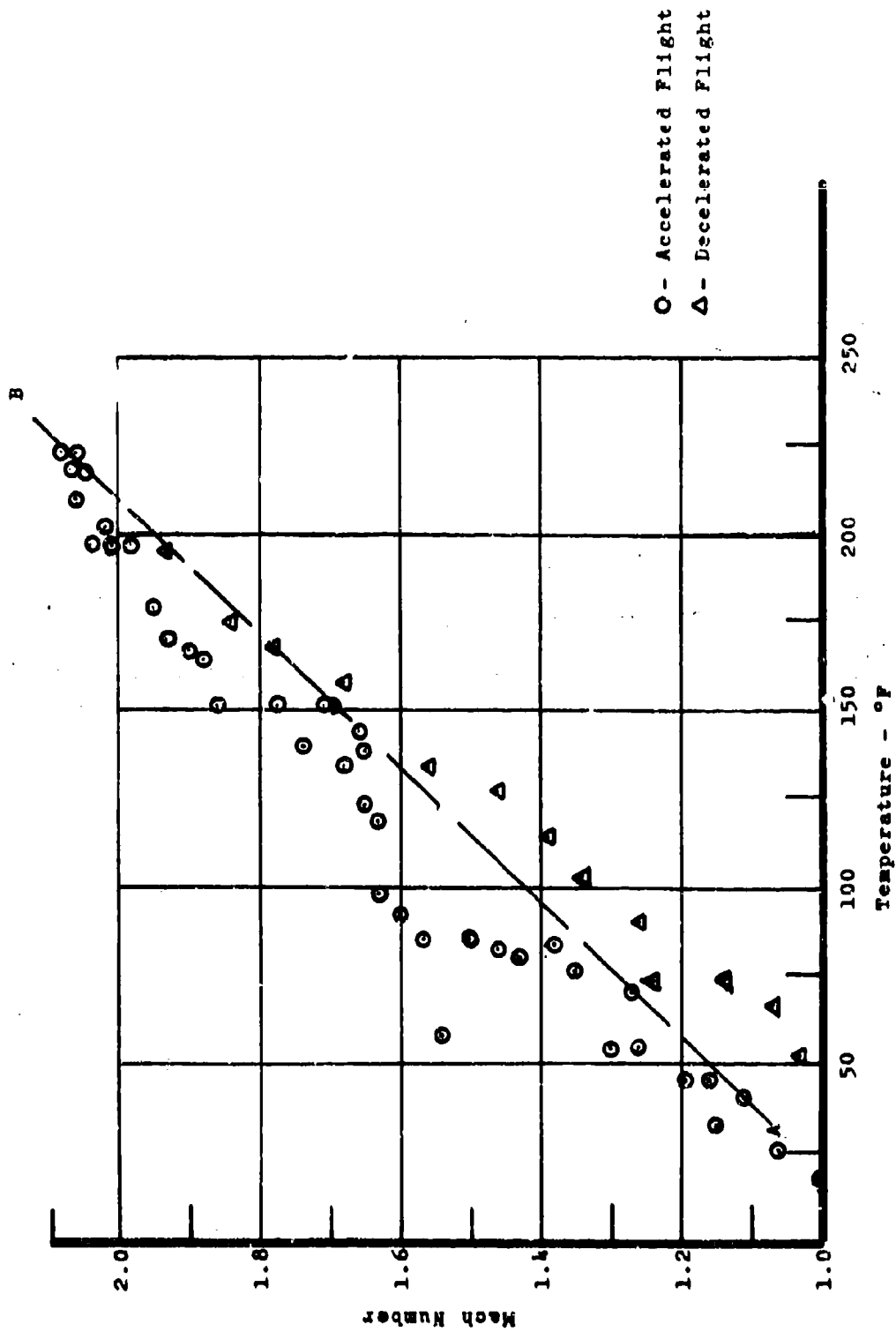


Figure 16. Mach Number Temperature Profile, Fuselage Station 340, Flight 37, B-58A

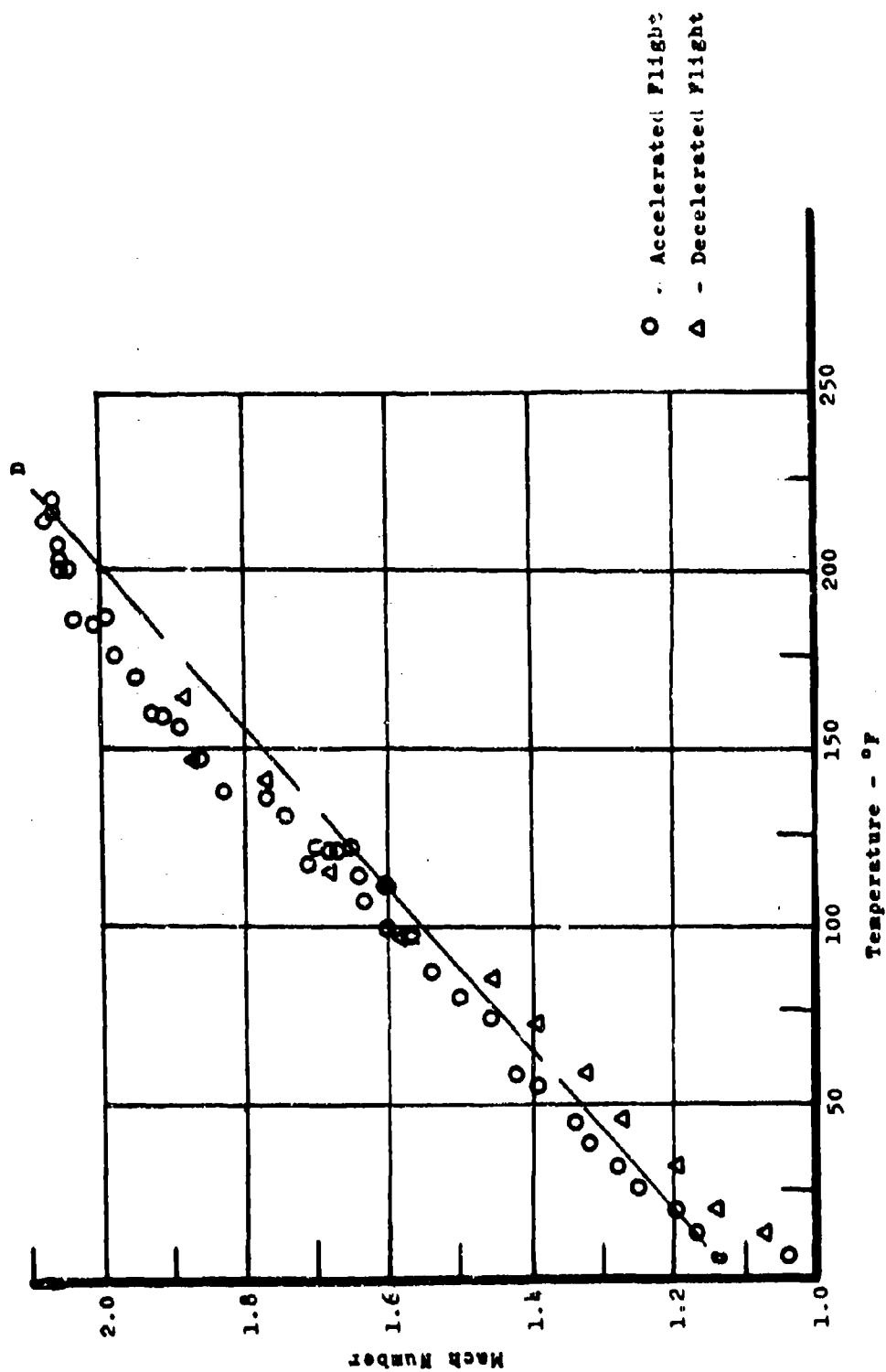


Figure 17. Mach Number Temperature Profile, Wing Station 200, Flight 37, B-58A

- O - Upper Spar Cap
 - Δ - Lower Spar Cap
 - ▽ - Leading Edge Flaps
 - X - Nose Boom
- Altitude - 41,400'

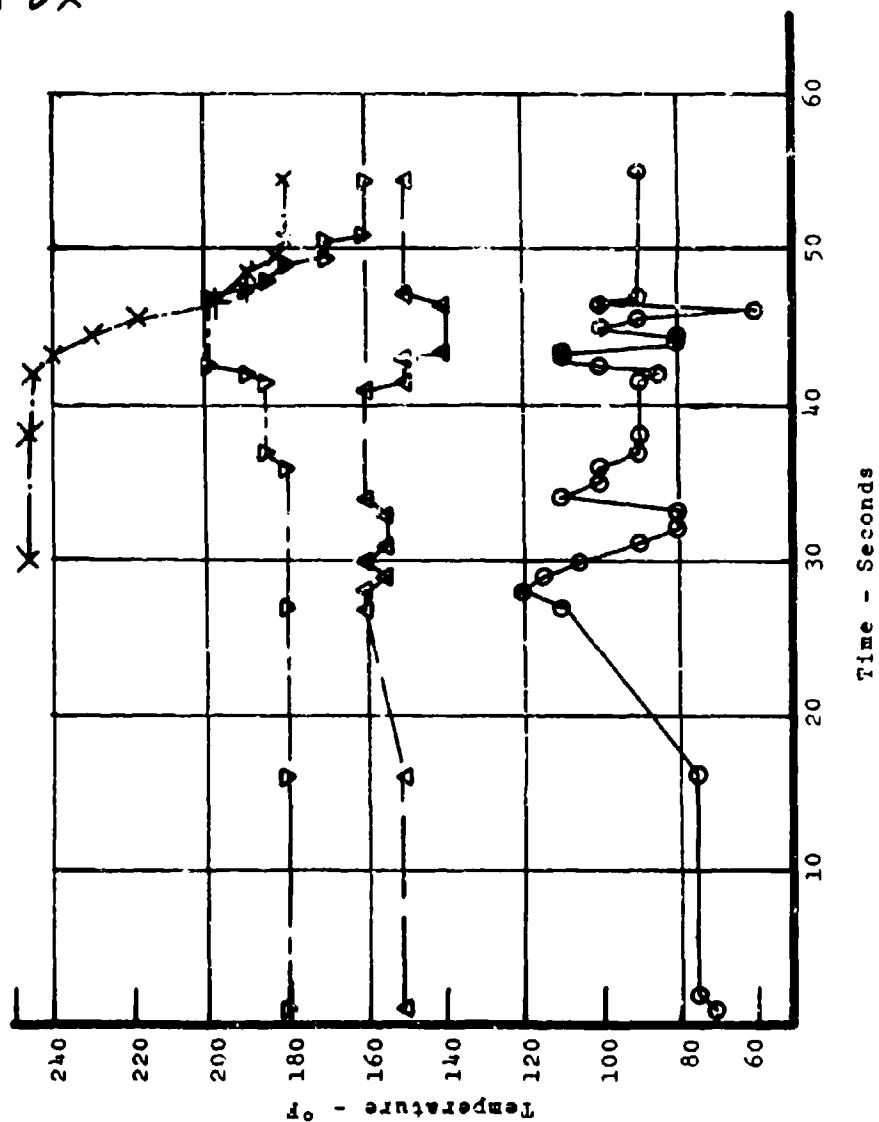


Figure 18. Temperature Time Profile, Wing and Nose Boom, Flight 21F-4, F-105D

- - Upper Spar Cap
 - △ - Lower Spar Cap
 - ▽ - Leading Edge Flaps
 - × - Nose Boom
- Altitude - 41,400'

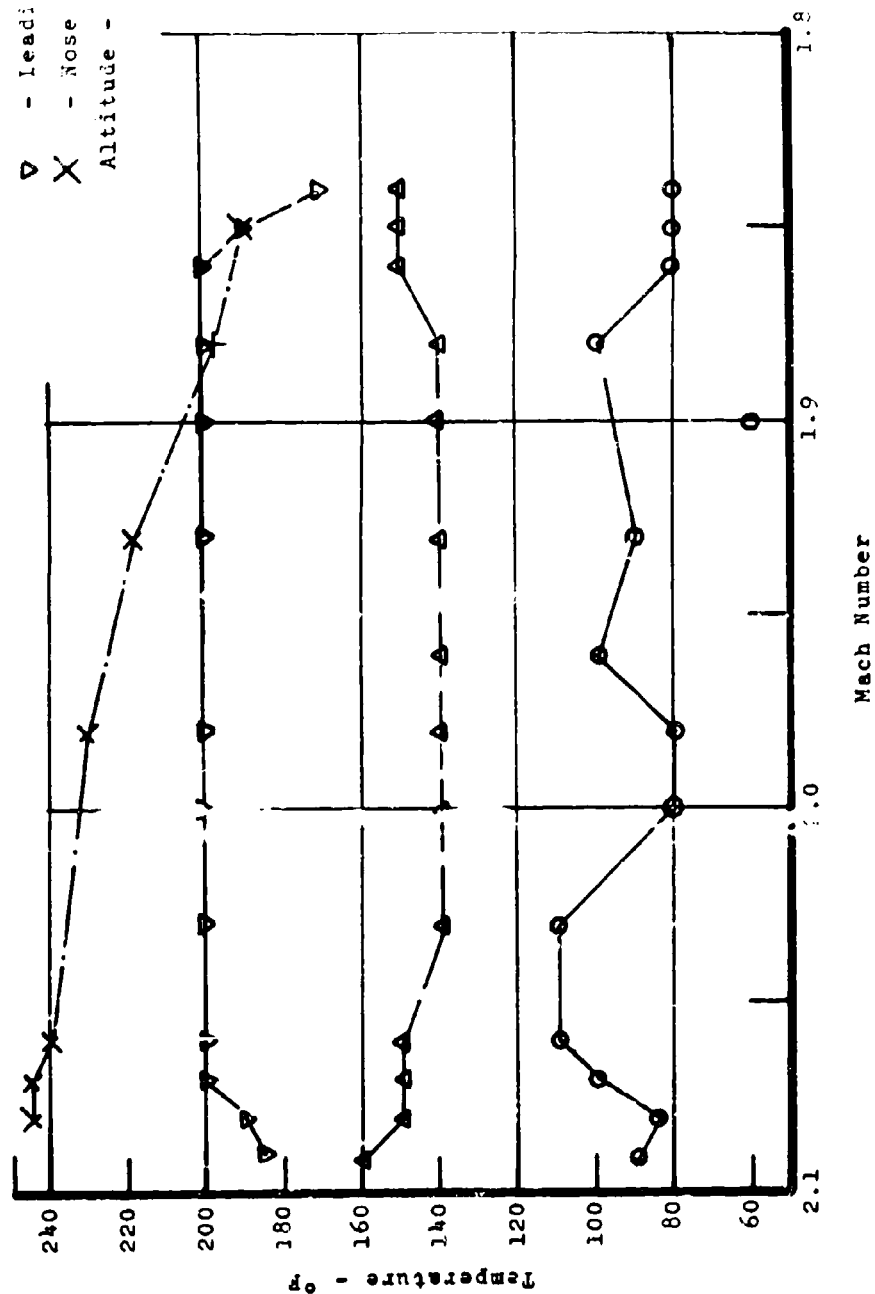


Figure 19. Temperature Mach Number Profile, Wing and Nose Boom, Flight 21F-4, F-105

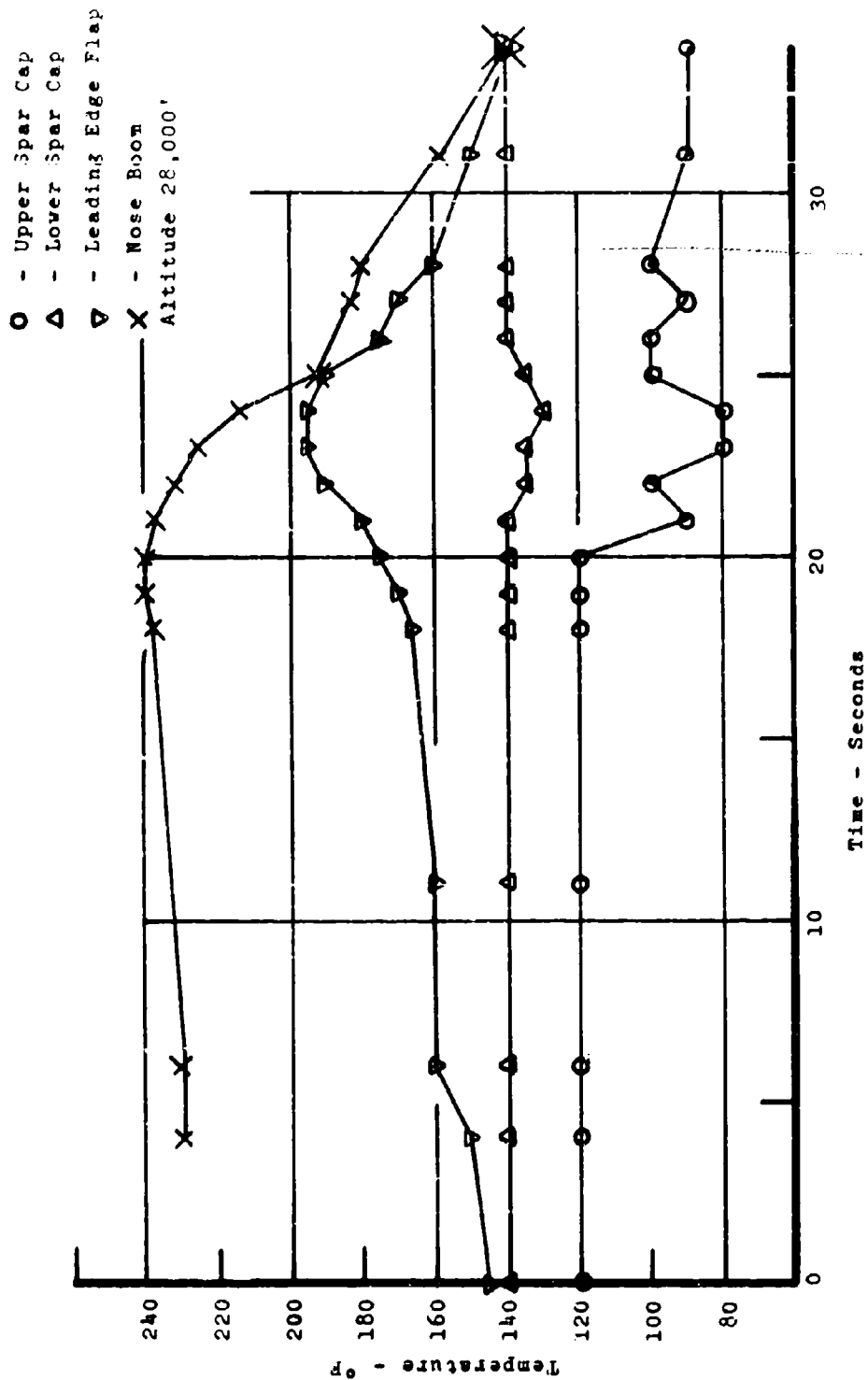


Figure 20. Temperature Time Profile, Wing and Nose Boom, Flight 21F-5, F-105D

- O - Upper Spar Cap
 - Δ - Lower Spar Cap
 - ▽ - Leading Edge Flaps
 - X - Nose Boom
- Altitude 28,000'

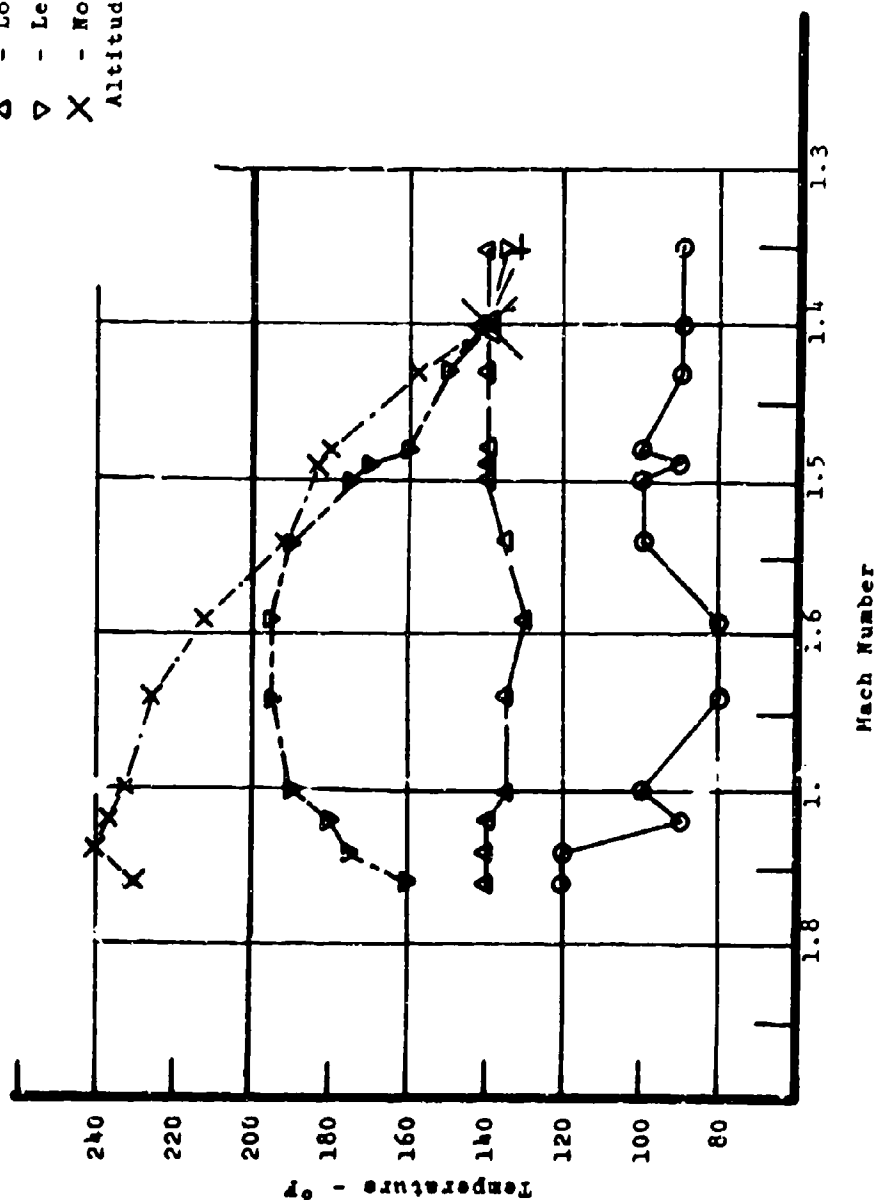


Figure 21. Temperature Mach Number Profile, Wing and Nose Boom, Flight 21F-5, P-105D

APPENDIX II

B-58A Aircraft Temperature Prediction Procedure

Temperatures were predicted using an IBM 704 digital computer programmed to solve the one dimensional composite wall problem with transient boundary conditions. The major input items to the computer were: (1) thickness and thermophysical properties of the various elements of the composite wall; (2) flight profile data, i.e. free stream pressure, velocity and temperature; (3) local pressure and velocity ratio; (4) time interval covered by the portion of the flight to be analyzed; and (5) time interval for which the finite difference computations are to be made.

The thermophysical properties of the honeycomb core were determined in the contractor test laboratories and reported in the contractors report CVAC FT6-1356. The flight profile data were fed into the computer from an auxiliary program which prepared the flight profile tape by curve fitting the ambient pressure, temperature and Mach number data and providing as output data the pressure, temperature and velocity at small time intervals. Mach number and free stream pressure were obtained from indicated air speed and pressure altitude. Data from several radiosonde weather observation stations within the flight corridor were analyzed to obtain the best geographical and chronological values of free stream air temperature.

The local heat transfer coefficient was computed within the main program using a modified flat plate equation, as shown in WADC TR 54-70, for all areas except the wing leading edge. NACA TN 3513 and NACA TN 3986 were used to compute leading edge heat transfer and to account for the effects of yaw. The local pressure and velocity ratios were computed from data taken from wind tunnel model tests at various Mach numbers and angles of attack.

The results of these computer programs are presented as temperature prediction curves in Figures 4 through 8 and 10 through 15.

APPENDIX III

Heat Balance Equations, F-105B

Where airplane skins and structures are adjacent to engine compartments, these elements are heated on their inner surface by the engine and become hotter than the adiabatic wall temperature. Similarly, structure located between the engine and the airplane skin will attain temperatures that must be higher than skin temperatures. To reduce structural components temperature to allowable temperature limits, insulation and cooling air are utilized.

To determine the temperature of the airframe from engine induced heat, heat balance equations are used (Reference 6).

One sample will be given herein, for computing the temperature on the fuel cell floor at fuselage station 553 to 581 (Figure A-1). The fuel cell floor is insulated and air cooled to prevent excessive fuel cell temperatures when empty. The heat balance on this section consists of the following equations: (t_3) is the temperature on fuel cell floor.

1. $Q_1 + Q_3 + Q_5 = Q_4$ heat balance on airplane skin
2. $Q_7 = Q_8 + Q_9$ heat balance on lower surface of
fuel cell support insulation
3. $Q_2 + Q_8 = Q_3 + Q_6$ heat balance on engine cooling air
4. $Q_9 = Q_{10} + Q_{11}$ heat balance on upper surface of fuel
cell support insulation

5. $Q_{10} = Q_{12}$ heat balance on fuel cell floor
 6. $Q_{11} + Q_{12} = Q_{13}$ heat balance on tank cooling air

- Q_1 = radiation from engine to skin
 Q_2 = convection from engine to air
 Q_3 = convection from air to skin
 Q_4 = convection from skin to boundary layer
 Q_5 = total radiation to skin
 Q_6 = heat gained by engine cooling air
 Q_7 = radiation from engine to fuel cell floor support insulation
 Q_8 = convection from fuel cell floor support insulation to engine cooling air
 Q_9 = conduction through insulation
 Q_{10} = radiation from fuel cell floor support insulation to fuel cell floor
 Q_{11} = convection from fuel cell floor support insulation to tank cooling air
 Q_{12} = convection from fuel cell floor to tank cooling air
 Q_{13} = heat gained by tank cooling air

$$Q_1 = FE FA h A(t_e - t_s)$$

$$A_e = 3/4 \times \frac{2\pi \times 18(581-553)}{144} = 16.5 \text{ ft.}^2$$

$$A_s = 28.8 \text{ ft.}^2$$

$$FE = \frac{1}{1/.6 + \frac{16.5}{28.8}(1/.6 - 1)} = .488; FA = 1$$

$$t_e = 735^\circ F \quad h = 6.2$$

$$Q_1 = .488 \times 6.2 \times 16.5 (735 - t_s) \\ = 49.9 (735 - t_s)$$

$$Q_2 = hA_e(t_e - \frac{t_{a4} + 260}{2}) \quad h = 1.5$$

$$A_e = \frac{4}{3} \times 16.5 = 22.0 \text{ ft.}^2$$

$$Q_2 = 1.5 \times 22.0 (735 - \frac{t_{a4} + 260}{2})$$

$$= 33(735 - \frac{t_{a4} + 260}{2})$$

$$Q_3 = hA_s (\frac{t_{a4} + 260}{2} - t_s)$$

$$= 1.5 \times 28.8 (\frac{t_{a4} + 260}{2} - t_s)$$

$$= 43.2 (\frac{t_{a4} + 260}{2} - t_s)$$

$$Q_4 = hA_s (t_s - t_{BL}) \quad h = 31$$

$$Q_4 = 31 \times 28.8 (t_s - 215)$$

$$= 893 (t_s - 215)$$

$$Q_5 = h A_s t_s \quad h = 0.76$$

$$= .76 \times 28.8 \times 248$$

$$= 5430$$

$$Q_6 = 778 (t_{a4} - 260)$$

$$Q_7 = FE FA h A_e (t_e - t_1)$$

$$A_e = 1/5 \times 22.0 = 4.4$$

$$A_1 = \frac{56 \times 28}{144} = 10.9 \text{ ft}^2$$

$$FE = \frac{1}{\frac{1.0}{.6} + \frac{4.4}{10.9} (\frac{1}{.6} - 1)} = .517, FA = 1, h = 10$$

$$Q_7 = .517 \times 10 \times 4.4 (735 - t_1)$$

$$= 22.8 (735 - t_1)$$

$$Q_8 = h A_1 (t_1 - \frac{t_{a4} + 260}{2})$$

$$= 1.5 \times 10.9 (t_1 - \frac{t_{a4} + 260}{2})$$

$$= 16.4 (t_1 - \frac{t_{a4} + 260}{2})$$

$$Q_9 = K A (t_1 - t_2) \quad K = .47/.55 \quad A = 10.9 \text{ ft}^2$$

$$Q_9 = \frac{.47}{.55} \times 10.9 (t_1 - t_2)$$

$$= 9.3 (t_1 - t_2)$$

$$Q_{10} = FE FA h A (t_2 - t_3)$$

$$FE = \frac{1}{\frac{1}{.6} + (\frac{1}{.6} - 1)} = .428, FA = 1, h = 3.2$$

$$Q_{10} = .428 \times 3.2 \times 10.9 (t_2 - t_3)$$

$$= 15.0 (t_2 - t_3)$$

$$Q_{11} = hA (t_2 - \frac{tc2 + 250}{2}) \quad A = 10.9 \text{ ft.}^2, h = 2.0$$

$$\text{Flow area} = 0.92 \text{ ft.}^2$$

$$G = \frac{W}{A} = \frac{.15}{.92} = .163 \text{ lb./sec. ft.}^2$$

$$Q_{11} = 2.0 \times 10.9 (t_2 - \frac{tc2 + 250}{2})$$

$$= 2.0 \times 10.9 (t_2 - \frac{tc2 + 250}{2})$$

$$Q_{12} = h A (t_3 - \frac{tc2 + 250}{2})$$

$$= 2.0 \times 10.9 (t_3 - \frac{tc2 + 250}{2})$$

$$= 21.8 (t_3 - \frac{tc2 + 250}{2})$$

$$Q_{13} = W C_p (tc2 - 250)$$

$$= .15 \times 3600 \times .24 (tc2 - 250)$$

$$= 130 (tc2 - 250)$$

The above solutions provided the necessary information for solution of basic heat balance equations 1 through 6.

This yielded the desired temperature on the fuel cell floor (t_2) as noted in Figure A-1.

LIST OF SYMBOLS

- Q = heat flow - BTU/hr.
- h = thermal conductance - BTU/hr.-ft.²-°F
- FE = emissivity factor
- FA = configuration factor
- K = thermal conductivity - $\frac{\text{BTU-ft.}}{\text{hr.-ft}^2\text{-°F}}$
- A = inlet area, in.²
- t_e = average engine temperature
- A_e = engine surface area
- A_s = skin surface area
- C_p = heat capacity - $\frac{\text{BTU}}{\text{lb.-°F}}$
- t_j = temperature on fuel cell floor

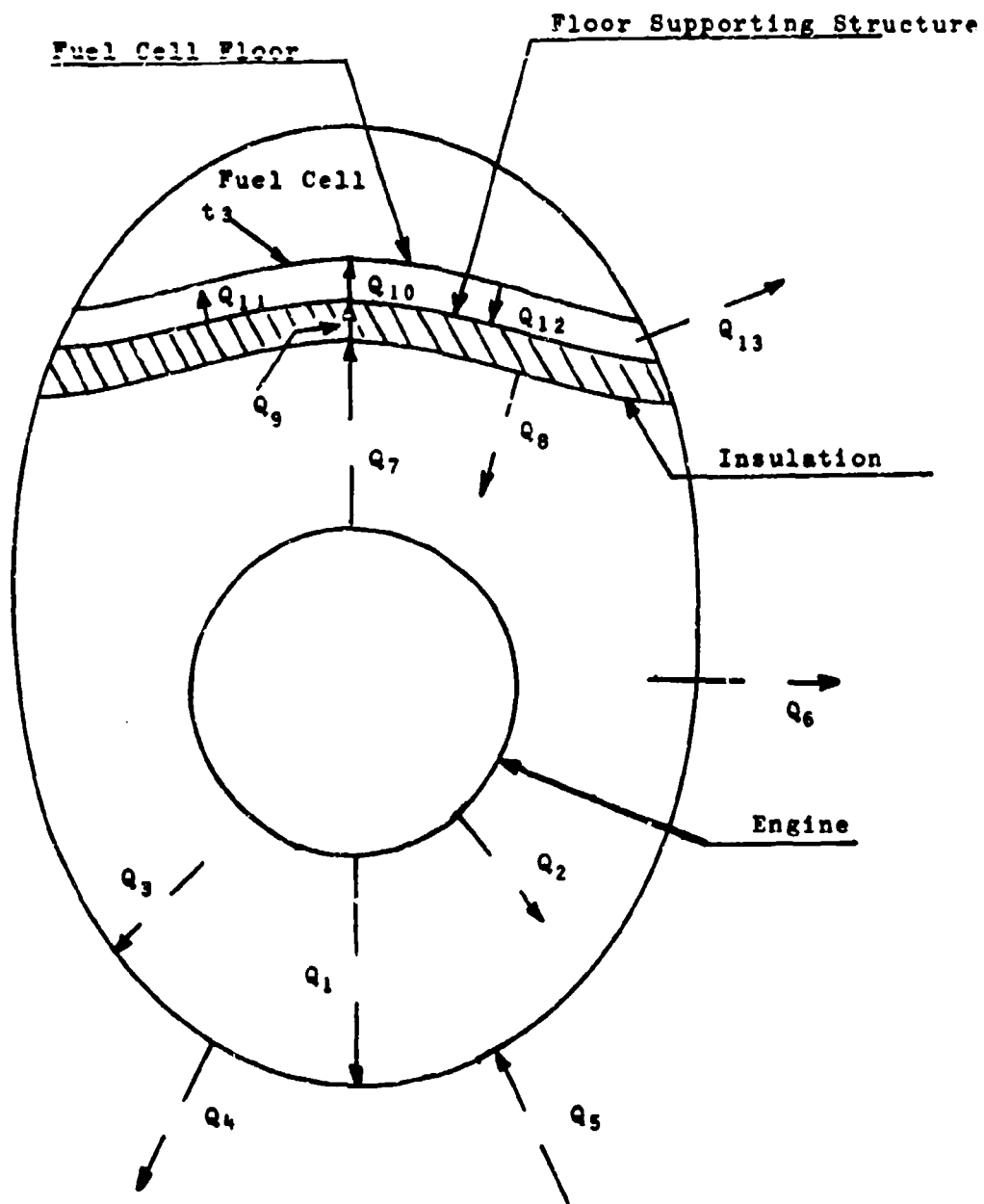


Figure A-1. Fuel Cell Floor Fuselage Station 553-581

UNCLASSIFIED

Security Classification

DOCUMENT CONTROL DATA - R&D		
(Security classification of title, body of abstract and indexing annotation must be entered when the overall report is classified)		
1. ORIGINATING ACTIVITY (Corporate author)		2a. REPORT SECURITY CLASSIFICATION
FDTR		Unclassified
		2b. GROUP
		N/A
3. REPORT TITLE		
Structural Temperatures at Supersonic Flight From B-58A and F-105D Aircraft		
4. DESCRIPTIVE NOTES (Type of report and inclusive dates)		
Final		
5. AUTHOR(S) (Last name, first name, initial)		
Durkee, Eugene D.		
6. REPORT DATE	7a. TOTAL NO. OF PAGES	7b. NO. OF REFS
November 1965	61	10
8a. CONTRACT OR GRANT NO.		8b. ORIGINATOR'S REPORT NUMBER(S)
a. PROJECT NO. 1367		AFDDL-TR-65-162
c. Task No. 136T17		
d.		8c. OTHER REPORT NO(S) (Any other numbers that may be assigned this report)
		None
9. AVAILABILITY/LIMITATION NOTICES Qualified requesters may obtain cys of this report fr ODU. This document is subject to special export controls and each transmittal to foreign nationals may be made only with prior approval of the Structures Division, (FDT) Air Force Flight Dynamics Laboratory, Wright-Patterson AFB, Ohio.		
11. SUPPLEMENTARY NOTES		12. SPONSORING MILITARY ACTIVITY
		AF Flight Dynamics Laboratory Research and Technology Division Wright-Patterson AFB, Ohio
13. ABSTRACT		
This report presents supersonic flight data from an instrumented B-58A and F-105D aircraft. These data comprise supersonic Mach number, altitude and recorded and predicted temperatures at various wing and fuselage stations. Data presentation is in the form of curves, plots and tables with pertinent descriptive information. These findings are presented herein to provide a basis for extending the state-of-the-art in structural design criteria for current and future flight vehicles.		

DD FORM 1473
1 JAN 64

UNCLASSIFIED

Security Classification

